

The theory of nucleosynthesis in stars: the slow neutron capture process

V. P. Chechev and Ya. M. Kramarovskii

V. G. Khlopin Radium Institute, Leningrad
Usp. Fiz. Nauk 134, 431-467 (July 1981)

The theory of the s process of nucleosynthesis has received considerable development during recent years, mainly as the result of more detailed physical and mathematical treatments and also as a result of the accumulation of new observational data on stellar evolution and the abundance of the elements in the solar system, and accumulation of experimental data on neutron-capture cross sections. The exact solution of the s-process equations obtained recently by Newman (1978) is discussed. It confirms the correctness of the initial s-process theory (Clayton, Fowler, Hull, and Zimmerman, 1961). At the same time for small neutron exposures the exact and initial solutions differ. The influence of branching of the s process due to competition between β decay and neutron capture is analyzed; it is noted that at a temperature $\sim 3 \cdot 10^8$ K and a density of free neutrons $1.6 \cdot 10^7$ cm⁻³ the s-process theory is in good agreement with observational data on the yields of the various nuclides. Models are discussed for the pulsed neutron s process, which leads to formation of heavy elements in the interior of a star as the result of periodic flares of the helium shell and subsequent remixing of the material.

PACS numbers: 97.10.Cv, 95.30.Cq

CONTENTS

Introduction	566
1. Astrophysical preconditions of the s process	567
2. The unbranched s process. Classical theory	569
a) Qualitative discussion. b) The theory of Clayton, Fowler, Hull, and Zimmerman. c) Exact solution. d) Comparison with experiment. e) The pulsed s process	
3. Branching of the s process	575
4. Thermodynamic conditions of the s process	578
5. Chronology of the s process	580
6. Termination of the s process	581
Brief conclusions	582
References	583

"The most incomprehensible thing about the world is that it is comprehensible."

A. Einstein

INTRODUCTION

According to current ideas the formation of the chemical elements in nature (nucleosynthesis) occurred in various processes in several stages: 1) cosmological nucleosynthesis in a hot Universe, 2) synthesis of elements in stars, 3) nucleosynthesis under the action of cosmic rays.

During the expansion of the Universe from the hot dense stage during the first three minutes the lightest elements were synthesized, mainly helium 4 and significantly smaller quantities of deuterium and helium 3. The observed yield of helium 4 is in good agreement with calculations according to the hot model.¹⁻⁴ At the same time this model cannot satisfactorily explain the synthesis of heavier elements, since the density and temperature dropped rapidly on expansion of the Universe.

Further synthesis of elements occurs in the interior

of stars of the first generation (Ref. 5).¹⁾ This stage is classified into two types: hydrostatic and explosive nucleosynthesis.⁶

Hydrostatic nucleosynthesis occurs during the evolution of stationary stars and is due to the burning in them of hydrogen, helium, and heavier elements. Helium 4 of cosmological origin together with helium produced as the result of burning of hydrogen is transformed into carbon 12, which can serve as the source material for synthesis of oxygen and silicon.

At higher temperatures ($\geq 10^9$ K) fusion of oxygen and silicon nuclei is possible. Here the capture of charged

¹⁾Here we are not discussing the synthesis of the light elements, which can occur in stars in slow processes, for example, in $p+p$ reactions. Our problem is to consider slow processes of neutron capture which lead to synthesis of elements heavier than iron.

particles turns out to be in equilibrium with the inverse reactions of photo-disintegration (the e process of nucleosynthesis⁷). They lead to formation of iron (^{56}Fe) and elements near it under conditions of thermodynamic equilibrium. Here in a slowly evolving star the temperature of the medium rises not too rapidly, so that the synthesis reactions occur at the lowest temperature at which they are efficient.

If the temperature of the material rises rapidly to much higher values, then the burning of carbon, oxygen, and silicon begins to occur explosively. In this case (explosive nucleosynthesis) the final products of the burning will differ from the products of hydrostatic nucleosynthesis. In an explosion when the temperature reaches $4 \cdot 10^9$ K the matter will consist almost completely of iron and its neighboring elements in the periodic table.

Iron nuclei are characterized by the maximum binding energy per nucleon. Energetically this is the most stable nucleus, and therefore the existence of elements heavier than iron cannot be explained by thermonuclear fusion reactions. Synthesis of these elements in such reactions would occur already not with an energy release, but with a significant expenditure of energy, and in addition, nuclear reactions in which a large number of light elements take part have an extremely low probability.

Suess and Urey⁸ proposed, and the Burbidges and Fowler and Hoyle⁹ showed in detail, that synthesis of heavy elements can occur by means of capture of free neutrons by two different routes, which have received the name the s and r processes.

The r process is the rapid successive capture of a large number of neutrons preceding β decay. It takes place only at sufficiently high neutron flux densities (10^{27} – 10^{40} neutrons/cm²/sec) in the explosions of supernovae when there is an outburst of stellar layers heated by a shock wave and containing the initial material of lighter elements.

The s process is the slow capture of neutrons in which the unstable nuclei formed decay before the next neutron can be added. This process is characterized by moderate neutron flux densities (10^{15} – 10^{16} neutrons/cm²/sec) and is possible in burning of the helium and carbon shells of massive stars and red giants, and in pulsed processes also in stars of intermediate mass.

Of the two neutron-capture processes, the s process is more suitable for detailed investigation under laboratory conditions, since the main link in the chain of the s process (neutron capture with subsequent β decay) is easily modeled experimentally. This is one of the reasons why the theory of the s process is more completely developed at the present time than the theory of rapid neutron capture.

1. ASTROPHYSICAL PRECONDITIONS OF THE s PROCESS

There are observational reasons to consider that in most stars of the main sequence (in particular, in the

Sun) the chemical composition of their atmospheres is close to the initial composition, i.e., to the composition of the interstellar medium from which they were formed. The chemical composition of the Sun is very similar to the composition of the Earth and of the meteorites (if we neglect the loss of volatile gases). At the same time the oldest of the known stars—the subdwarfs, which were formed in the earliest stages of the history of the Galaxy—contain less of the heavy elements than does the Sun.¹⁰

This permits us to suggest that the substantial quantity of heavy elements which is observed in young stars was synthesized soon after the formation of the Galaxy in the interiors of massive stars of the first generation in the course of their rapid evolution (~100 million years), which was terminated by outbursts of supernovae. Apparently at the beginning of the evolution of the Galaxy the frequency of explosions of supernovae was much greater than at the present time. In explosions of supernovae a substantial quantity of their matter is ejected into the interstellar medium, and this is then mixed with the interstellar gas. Matter ejected from first-generation stars subsequently served as the material for formation of stars of the second generation (including the Sun).²⁾ The chemical composition of the future solar system could also change partly, being enriched in the heavy elements as the result of explosion of a supernova in the immediate vicinity of the Sun.¹¹

The final chemical composition of the ejected material is affected much more strongly by nucleosynthesis processes which occur at the moment of explosion of a supernova and which are due to intense neutron fluxes, than they are affected by nuclear reactions occurring in the star before the explosion. Here the main process of nucleosynthesis at the moment of the explosion, which is characterized by times of 1–100 sec, is the r process.³⁾

In the present section we cannot discuss all the preconditions related to the synthesis of heavy elements and shall limit ourselves to a qualitative analysis of the astrophysical conditions of the s process. A detailed analysis of the contemporary situation, of where and under what conditions the slow capture of neutrons has

²⁾Spectroscopic observations in the ultraviolet region on rockets and satellites show that massive hot stars lose a significant part of their mass. The material ejected into the interstellar medium and which mixes with it can contain chemical elements produced in the s process. In the last stages of evolution of red giants a significant loss of their mass also occurs as the result of ejection of material from the outer shell. A strong argument in favor of this, as pointed out by I. S. Shklovskii,¹⁰ is the observations of dense gaseous formations surrounding hot stars of low luminosity—so-called planetary clouds.

³⁾Several authors¹²⁻¹⁴ have suggested a mechanism of formation of the heavy elements in neutron stars at high neutron concentrations ($n_n > 10^{30}$ cm⁻³). Still another model involving the role of neutron stars in nucleosynthesis assumes destruction of a neutron star in a close binary system if the second of the components is a black hole with a large mass.⁴⁹

occurred and is occurring with formation of heavy elements, is given in the review of Virginia Trimble.¹⁵

Nuclear theory dictates the conditions under which the s process can be encountered, and astrophysics determines the location appropriate for it. The thermodynamic conditions of slow nucleosynthesis processes permit us to assume that they are accomplished in the normal stage of evolution of stars.

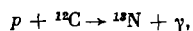
For a star passing through the normal evolutionary path there are three characteristic times during which its properties can change substantially: 1) the dynamic characteristic time $t_d \approx (2r_s^3/GM_s)^{1/2} \sim 10^3 - 10^4$ sec is the time which is required by the star for readjustment (explosion) if the balance between gravitational forces and pressure forces is destroyed in it; 2) the thermal characteristic time $t_t \approx GM_s^2/L_s r_s \approx 10^4$ years⁴¹ is the time for which the gravitational energy of a star can maintain its luminosity L_s without participation of nuclear energy sources; 3) the nuclear characteristic time $t_n \approx E_n/L_s$ is the total time of existence of a star with a given luminosity, which depends on the supply of thermonuclear fuel. For most stars $t_n \gg t_t \gg t_d$.

In the s process each nucleus of the iron peak in formation of heavier nuclides captures ≈ 100 neutrons, and the time between two successive neutron capture events is greater than the time of β decay. If the neutrons appear in the stationary stage of evolution occurring within the thermal or nuclear times, β decay of unstable nuclei (with lifetimes less than 10^3 years) can occur between successive neutron captures, i.e., the s process will unavoidably occur. It is clear from this that the duration of this process is characterized by times $\geq 10^3$ years.

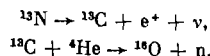
Where does the s process develop? The location of the s process must have appropriate thermodynamic conditions for it to occur, i.e., a temperature sufficient for occurrence of nuclear reactions liberating neutrons ($\geq 10^8$ K), a neutron flux density $\sim 10^{15} - 10^{18}$ neutrons/cm²/sec, and a duration of the irradiation $\sim 10^3$ years. In addition one can indicate two further principal astrophysical circumstances for development of the s process¹⁵: a) the products of the s process must be carried out to the surface of the star in which they are produced, in order that they can be observed (as occurs in carbon-hydrogen red giants, barium stars, and so forth); b) the products of the s process must enter the interstellar medium without further nuclear reactions.

In order to transport material to the surface of a star, convection or mixing is necessary. Mixing also is necessary to explain the sources of neutrons.

If hydrogen from the outer layers penetrates into regions containing helium and carbon, then in such stars there can occur reactions liberating neutrons,¹⁶ which are necessary for the s process:



⁴¹Here M_s and r_s are respectively the mass and radius of the star and G is the gravitational constant.



The reaction ${}^{13}\text{C}(\alpha, n){}^{16}\text{O}$ occurs at temperatures $\approx 10^8$ K.

At temperatures $T \geq 10^9$ K free neutrons can also arise in exothermal (α, n) reactions in nuclei with mass numbers $A = 4n + 1 > 13$ (${}^{17}\text{O}$, ${}^{21}\text{Ne}$, ${}^{25}\text{Mg}$). Burning of carbon at these temperatures produces a substantial number of neutrons: ${}^{12}\text{C}({}^{12}\text{C}, n){}^{23}\text{Mg}$ produces 5–25 neutrons per iron nucleus. Burning of oxygen (${}^{16}\text{O} + {}^{16}\text{O} \rightarrow {}^{31}\text{Si} + n$) leads to a yield already of ~ 100 neutrons per ${}^{56}\text{Fe}$ nucleus.

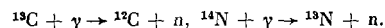
We might therefore assume that (α, n) reactions in the nuclei ${}^{13}\text{C}$, ${}^{17}\text{O}$, ${}^{21}\text{Ne}$, and ${}^{25}\text{Mg}$ are the main sources of free neutrons at the temperatures associated with the hydrostatic phases of stellar evolution. Unfortunately, the yields of these nuclei after burning of hydrogen in the CNO cycle are small (${}^{13}\text{C}/{}^{56}\text{Fe} \sim 0.2$). The principal element formed in this cycle is ${}^{14}\text{N}$, which actively absorbs neutrons by the reaction ${}^{14}\text{N}(n, p){}^{14}\text{C}$. Therefore additional mechanisms (or models) are necessary for the formation of these nuclei in the burning helium shell itself or transportation of them there by means of mixing.

As was shown by Schwarzschild and Härm,⁴⁰ such mixing actually occurs in the phase of stellar evolution in which hydrogen and helium burn in thin shells around an inert core. Such burning in stars of intermediate and low masses makes them in some degree unstable, which leads to appearance of thermal pulsations³⁹ in which the rate of generation of energy increases rapidly for several years. These pulsations give way to extended quiet phases of stellar evolution ($\geq 10^3$ years). During the pulsations the convective shell containing ${}^{12}\text{C}$ nuclei produced in burning of helium mixes with the hydrogen-helium shell, thereby providing conditions for formation of sufficient quantities of ${}^{13}\text{C}$ nuclei and intense occurrence of the reaction ${}^{13}\text{C}(\alpha, n)$ [for more detail see section (e) of chapter 2].

This pulsation mechanism provides the s-process conditions for an extensive class of stars of intermediate and large masses—from $3M_{\odot}$ to $10M_{\odot}$.

Cameron⁴⁷ has pointed out the possibility of an additional neutron source which is obtained in burning helium by means of the following reactions: ${}^{14}\text{N}(\alpha, \gamma){}^{18}\text{F}(e^+, \nu){}^{18}\text{O}(\alpha, \gamma){}^{22}\text{Ne}(\alpha, n){}^{25}\text{Mg}$. Temperatures sufficient for intense occurrence of these reactions ($\geq 3 \cdot 10^8$ K) are achieved in burning of helium nuclei in very massive stars ($\geq 9M_{\odot}$)^{50,51} or in burning of the helium shell in stars of smaller mass ($\sim 2-8$ solar masses). For first-generation stars this mechanism provides about 20 neutrons per iron nucleus.

As Harrison and Edwards¹⁷ showed in 1974, another important source of free neutrons is provided by low-temperature photoneutron reactions which occur following (p, γ) reactions:



At $T \sim 10^8$ K these processes produce significant neutron fluxes ($10^9 - 10^{11}$ neutrons/cm²/sec), but these are in-

sufficient to provide the observed yield of elements in the s process of nucleosynthesis. Nevertheless photo-neutron cycles can be an important secondary source of free neutrons.

Thus, the s process is determined by neutrons which are liberated in nuclear reactions in the normal stage of evolution of stars. These can be either rather massive stars or, if we assume a pulsating nature of the evolution, stars of intermediate masses (~2-5 solar masses).

2. THE UNBRANCHED s PROCESS. CLASSICAL THEORY

a) Qualitative discussion

Figure 1 shows a universal abundance curve of the chemical elements in the solar system, constructed on the basis that the abundances in the Earth, meteorites, and Sun are similar. Peaks in the curve are distinguished at $A=56$ (the iron peak), $A=90$ (neutron number $N=50$), $A=138$ ($N=82$), and $A=208$ ($N=126$). This is the first qualitative indication of the involvement of neutron capture processes in nucleosynthesis, since these mass numbers correspond to nuclei with magic numbers of neutrons, which are more stable than their neighbors and have very small cross sections for capture of the next neutron. The paths of formation of elements in the s and r processes are shown in the $N-Z$ diagram of Fig. 2.

Since the s process consists of the slow capture of neutrons, we can expect that the yields of nuclei in the s process will be determined by their capture cross sections σ . For an established s process the contents

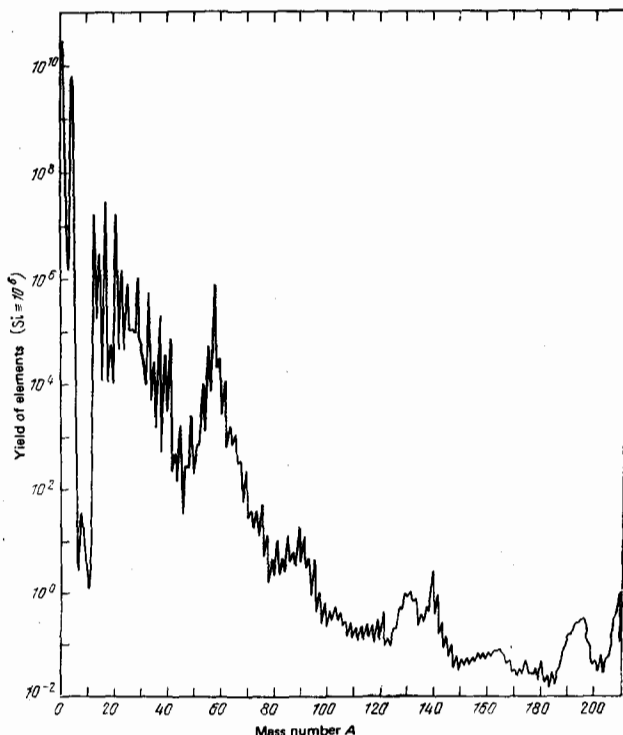


FIG. 1. Universal abundance curve of the chemical elements in the solar system.

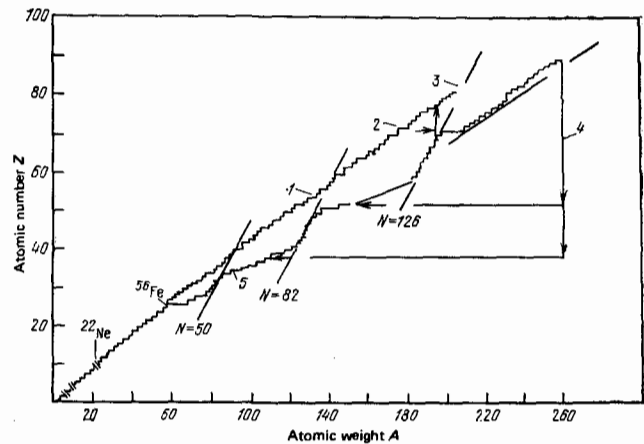


FIG. 2. Paths of formation of elements in the s and r processes in an $N-Z$ diagram. 1—Path of slow neutron capture (n, γ), 2 (---)—consecutive β decay, 3— α decay, 4—fission, 5—fast capture of neutrons (n, γ).

of nuclei neighboring in A in the s-process chain should be inversely proportional to σ . The larger the capture cross section, the smaller should be the yield of a given isotope. A quantitative proof of this fact is the abundance of the stable isotopes of tin and samarium, which we assume to be completely or partly produced in the s process:

$$\frac{N(^{148}\text{Sm})\sigma(^{148}\text{Sm})}{N(^{150}\text{Sm})\sigma(^{150}\text{Sm})} = 0.98 \pm 0.06,$$

$$\frac{N(^{116}\text{Sn})\sigma(^{116}\text{Sn})}{N(^{118}\text{Sn})\sigma(^{118}\text{Sn})} = 0.8 \pm 0.2,$$

$$\frac{N(^{130}\text{Sn})\sigma(^{130}\text{Sn})}{N(^{118}\text{Sn})\sigma(^{118}\text{Sn})} = 0.9 \pm 0.3.$$

As we can see, all these ratios are of the order of unity in accordance with the principal conclusion of the theory.

From this qualitative discussion it already follows that the s-process hypothesis predicts the existence of regions where the product σN is almost constant. It is confirmed by the experimental curve of $\sigma N = f(A)$ for the elements of the solar system (see Fig. 8 below), in which the steps corresponding to $\sigma N = \text{const}$ are easily visible.

A further important proof of involvement of the s process in nucleosynthesis is the observation in stellar spectra of the lines of technetium, of which there are no stable isotopes. The longest half-life of the technetium isotopes is that of technetium 99 ($T_{1/2} = 2.6 \cdot 10^6$ years). The duration of the existence of stars is considerably greater than this time, and consequently technetium must be produced in the star in whose spectrum it is observed. At the same time the half-life of ^{99}Tc is sufficiently great for it to be preserved in the chain of the s process.

b) The CFHZ theory

The initial formulation¹⁹ of the theory of the s process⁵⁾ defined the standard (canonical) path of the s

⁵⁾This formulation of the theory of the s process has become known in the physics literature as CFHZ (Clayton, Fowler, Hull, Zimmerman).

process on the assumption that the lifetime of the radioactive nuclei against β decay in the s-process chain is always less than the lifetimes for capture of the next neutron ($\lambda_\beta^{-1} < \lambda_n^{-1}$). This approach does not take into account the branching which is possible when long-lived isotopes are encountered on the main track of the s process, which prefer to capture a neutron rather than undergo β decay. A more complete theory of the s process must take into account the probability of branching, which introduces corresponding corrections to the calculations of the yields of nuclides in comparison with the standard theory. The influence of branching and the magnitude of these corrections will be discussed in the next section. Here we shall give the theory of the unbranched s process which develops along the main, canonical, path. An example of such an s process is given in Fig. 3.

Let us consider some region inside a star with a constant temperature T and a density of free neutrons $n_n(t)$ which does not change over the entire region but can depend on time. Let $N_A(t)$ be the yield of nuclei with mass number A in the track of the s process, σ_A be the cross section for neutron capture for these nuclei, and v be the velocity of the free neutrons which bombard the nuclei under discussion. Then for the yield of the nuclei N_A we have

$$\frac{dN_A}{dt} = \langle \sigma v \rangle_{A-1} n_n(t) N_{A-1} - \langle \sigma v \rangle_A n_n(t) N_A. \quad (1)$$

This is the basic equation of the theory of the s process, which takes into account the fundamental assumption that the β decays between isobars occur more rapidly than the neutron captures ($\lambda_\beta \gg \lambda_n$). The quantity $\langle \sigma v \rangle$ appears here as a necessary averaging associated with a Maxwellian distribution. Neutron capture in heavy nuclei occurs in close-lying overlapping levels of the compound nucleus. As a consequence of the Maxwellian distribution of neutrons (with energy $\sim kT$) it is difficult to obtain experimentally an energy resolution comparable with the distance between levels of the compound nucleus, and therefore measurements give σ and σv averaged over the entire energy region, and for this reason σ varies smoothly with neutron energy.

It is well known that at low neutron energies with a high degree of accuracy $\sigma \propto 1/v$. This dependence is preserved in the energy region of several tens of keV (stellar temperatures), where together with the s waves of neutron capture it is also necessary to take into account p waves. Consequently the quantity σv can be

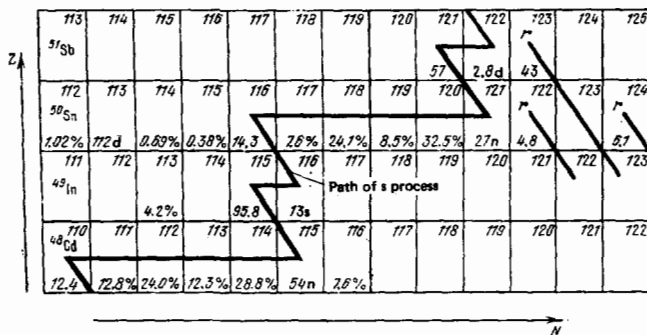


FIG. 3. Example of unbranched s process.

considered constant in the region of stellar temperatures, which permits use of σ and v in calculations for a single energy—the most probable energy—of the Maxwellian distribution: $\langle \sigma v \rangle = \sigma_T v_T$; here $\sigma_T = \sigma(kT)$, $v_T = (2kT/\mu)^{1/2}$, and μ is the reduced mass of the neutron in the center-of-mass system ($\mu \cong m_n$).

Equation (1) then goes over to

$$\frac{dN_A(t)}{dt} = v_T n_n(t) \sigma_{A-1}(kT) N_{A-1}(t) - v_T n_n(t) \sigma_A(kT) N_A(t). \quad (2)$$

We shall introduce a new independent variable which uniquely defines the total number of neutrons bombarding a unit of surface—the neutron exposure τ :

$$d\tau = n_n v_T dt, \quad \tau = \int n_n v_T dt. \quad (3)$$

If σ is expressed in millibarns, then the dimensions of the neutron exposure are $[\tau] = \text{mb}^{-1} = 10^{27} \text{ neutrons/cm}^2$.

Equation (2) with the new variable takes on the well known form

$$\frac{dN_A}{d\tau} = \sigma_{A-1} N_{A-1} - \sigma_A N_A. \quad (4)$$

Equation (4) is applicable only to the region of synthesized nuclei with mass number $57 \leq A \leq 209$. The lower limit is due to the fact that lighter elements are produced preferentially in reactions induced by charged particles. The upper limit is determined by the fact that when ^{209}Bi captures a neutron the isotopes eventually formed are those of lead, which undergo α decay, leading to a decrease of Z and A .

In the s process a group of initial nuclei is bombarded by an unknown number of neutrons, which determines the spread in the value of the neutron exposure τ . In addition, if we assume that the heavy elements of the solar system were synthesized in different locations and then were mixed long before the formation of the Sun and planets, they could be the product of s processes with different values of neutron exposure. The common solution for nuclear synthesis in this case is first to consider a neutron flux characterized by a given value of τ , and then to consider superposition of solutions for different τ values.

We shall choose as a seed nucleus in the s-process chain ^{56}Fe . Proceeding from Eq. (4), we can write down the following system of equations:

$$\left. \begin{aligned} \frac{dN_{56}}{d\tau} &= -\sigma_{56} N_{56}, \\ \frac{dN_A}{d\tau} &= \sigma_{A-1} N_{A-1} - \sigma_A N_A, \quad 57 \leq A \leq 209, \\ \frac{dN_{210}}{d\tau} &= \sigma_{210} N_{210}, \end{aligned} \right\} \quad (5)$$

with boundary conditions

$$N_A(0) = \begin{cases} N_{56}(0), & A = 56, \\ 0, & A > 56. \end{cases}$$

We shall introduce a more convenient notation: $k = A - 55$, $\psi_k(\tau) \equiv N_k N_k(\tau) / N_1(0)$. Then the set of differential equations describing the s process is written in the form

$$\left\{ \begin{aligned} \frac{d\psi_1}{d\tau} &= -\sigma_1 \psi_1(\tau), \\ \frac{d\psi_k}{d\tau} &= \sigma_k [\psi_{k-1}(\tau) - \psi_k(\tau)], \\ &2 \leq k \leq 154, \end{aligned} \right. \quad (6)$$

with boundary conditions $\psi_k(0) = \sigma_1 \delta_{1k}$, where δ_{1k} is the Kronecker symbol.

Since the cross sections σ_k are assumed to be independent of τ , the equations (6) can be integrated:

$$\begin{aligned} \psi_1(\tau) &= \sigma_1 \exp(-\sigma_1 \tau), \\ \psi_k(\tau) &= \sigma_k \int_0^\tau \psi_{k-1}(\tau') \exp[\sigma_k(\tau' - \tau)] d\tau'. \end{aligned} \quad (7)$$

Bateman²⁰ has shown that the solution of the system of equations (7) can be written in the form of a series expansion:

$$\psi_k(\tau) = \sum_{i=1}^k c_{ik} \exp(-\sigma_i \tau), \quad (8)$$

where

$$c_{ik} = \sigma_i \prod_{j=1}^k \frac{\sigma_j}{\sigma_j - \sigma_i}. \quad (9)$$

In obtaining an exact solution by means of this expansion a major difficulty arises as a result of the possible degeneracy of the quantities σ : for $\sigma_m = \sigma_n$, with $n \neq m$, the expansion loses meaning, whereas in practice many experimental cross sections σ_i are the same within experimental error (see Table I and its discussion). To overcome these difficulties it is necessary to carry out the limiting transition $\sigma_m \rightarrow \sigma_n$.

In addition, even if all cross sections σ_i are arbitrarily made slightly different, the numerical summation of the exact Bateman expansion presents great difficulties as a result of the cumbersome nature of the calculations. Before the advent of contemporary computers the numerical integration of the equations (7) was unachievable, and therefore satisfactory approximate methods were developed for calculation of the s process¹⁹ (the CFHZ theory).

Let us consider the main features of the CFHZ solution. Returning to Eq. (6), in accordance with CFHZ we shall use for the functions ψ_k the Laplace transforms $\bar{\psi}_k(s) = \int_0^\infty \psi_k(\tau) \exp(-s\tau) d\tau$. The equations (6) then go over into the form

$$\begin{cases} s\bar{\psi}_1(s) = \sigma_1 [1 - \bar{\psi}_1(s)], \\ s\bar{\psi}_k(s) = \sigma_k [\bar{\psi}_{k-1}(s) - \bar{\psi}_k(s)]. \end{cases} \quad (10)$$

From this we obtain

$$\bar{\psi}_k(s) = \prod_{i=1}^k \frac{\sigma_i}{s + \sigma_i} = \prod_{i=1}^k \frac{1}{(s/\sigma_i) + 1}. \quad (11)$$

The exact inversion of this Laplace function is too cumbersome. The problem is to find an approximate form of its inverse.

In the special case of constant cross sections equal to λ , we have

$$\bar{\psi}_m(s) = \frac{1}{((s/\lambda) + 1)^m}; \quad (12)$$

here $\bar{\psi}_m(s) = \lambda \bar{N}_m(0)/N_1(0)$, \bar{N}_m is the yield on the assumption of constancy of the cross sections, and m is a new numerical index similar to k .

The approximate solution of the correct inversion of the Laplace function (11) consists of choosing, for each k , values of m_k and λ_k in Eq. (12) such that

TABLE I.

Nuclides	Cross section σ from Ref. 21, mb	Cross section σ in mb, estimated value (present work*)	Yield N_g ($\text{Si} \approx 10^6$) (from Ref. 16)	σ/N_g , estimated value**
⁵⁶ Fe	13.75	13.7±1.7	7.61·10 ⁴	(104±25)·10 ⁴
⁵⁷ Fe	29.5	29.2±3.8	1.82·10 ⁴	(53±13)·10 ⁴
⁵⁸ Co	35	36±8	2.21·10 ⁴	(8±2)·10 ⁴
⁶⁰ Ni	19.25	19±9	1.26·10 ⁴	(24±12)·10 ⁴
⁶² Ni	26	26±5	1.76·10 ³	(4.6±1.3)·10 ³
⁶³ Cu	49	49±14	635	(3.1±1.1)·10 ⁴
⁶⁴ Ni	23	23±5	5.18·10 ³	(1.19±0.35)·10 ³
⁶⁵ Cu	42	42±7	284	(1.19±0.31)·10 ⁴
⁶⁴ Zn	50	50	732	(37±10)·10 ³
⁶⁶ Zn	23	23±3	278	(6.4±1.5)·10 ³
⁶⁹ Ga	130	130±30	29	(3.8±0.9)·10 ³
⁷⁰ Ge	84	84	25.8	(2.2±0.6)·10 ³
⁷¹ Ga	120	133±23	19	(2.5±0.7)·10 ³
⁷⁴ Ge	35	54±17	36	(1.9±0.7)·10 ³
⁷⁵ As	490	435±101	6.6	(2.9±0.9)·10 ³
⁷⁶ Se	100	100	6.32	(6.3±1.8)·10 ²
⁷⁸ Se	42.7	42.7	15.8	(6.8±1.9)·10 ²
⁸⁰ Se	38.5	43±21	33.5	(1.4±0.8)·10 ³
⁸¹ Br	460	460±80	6.68	(3.1±0.8)·10 ³
⁸² Kr	122	122	5.41	(6.6±1.9)·10 ²
⁸⁴ Kr	25	25	26.5	(6.7±1.9)·10 ²
⁸⁶ Rb	260.5	303.65	4.16	(2.0±0.6)·10 ³
⁸⁸ Sr	74	80±11	5.76	(4.6±1.1)·10 ²
⁸⁷ Sr	109	109±9	3.8	(4.1±0.9)·10 ²
⁸⁸ Sr	6.9	8.2±2.3	46.2	(3.8±1.3)·10 ³
⁸⁹ Y	21	21±4	3.0	63±17
⁹⁰ Zr	16.75	20.4±6.0	5.4	(1.1±0.4)·10 ³
⁹¹ Zr	68	68±8	3.14	(2.1±0.6)·10 ³
⁹² Zr	34	40±11	1.6	64±22
⁹⁴ Zr	20	20±2	2.4	48±11
⁹³ Mo	430	430±50	0.1	43±10
⁹⁶ Mo	97	95±6	0.42	40±7
⁹⁷ Mo	350	350±50	0.08	28±7
⁹⁸ Mo	126	100±38	0.44	44±19
⁹⁹ Ru	640	640	0.242	155±44
¹⁰⁰ Ru	110	110	0.202	22±6
¹⁰⁴ Pd	197	197	0.164	32±9
¹¹⁰ Cd	270	245±46	0.262	64±18
¹¹⁶ Sn	100	100±15	0.515	52±13
¹¹⁷ Sn	420	430±20	0.14	60±12
¹¹⁸ Sn	63	74±20	0.83	61±21
¹¹⁹ Sn	260	270±17	0.18	49±10
¹²⁰ Sn	50	50±15	1.21	60±12
¹²³ Te	270	270±30	0.164	44±10
¹²⁵ Te	820	820±30	0.054	44±9
¹²⁴ Te	150	150±20	0.31	46±9
¹²⁹ Te	430	430±30	0.12	52±11
¹²⁸ Te	70	73±20	0.42	31±10
¹³⁴ Xe	232	232	0.11	26±7
¹³⁰ Xe	143	143	0.21	30±8
¹³⁴ Ba	225	225±35	0.114	26±6
¹³⁶ Ba	75.5	67±21	0.367	25±9
¹³⁷ Ba	72.6	72.6	0.543	39±11
¹³⁸ La	44	44±4	0.24	10±2
¹⁴⁰ Ce	10	17±5	1.04	18±6
¹⁴² Nd	75.8	75.8	0.16	12±3
¹⁴⁶ Nd	105	105±16	0.134	14±4
¹⁴⁸ Sm	260	260±50	0.026	6.8±1.9
¹⁵⁰ Sm	370	370±70	0.017	6.3±1.7
¹⁵⁴ Gd	1164	1164±350	0.0073	8.5±3.1
¹⁶⁰ Dy	1010	1010	0.0083	8.4±2.4
¹⁶⁸ Er	243	243±73	0.0609	14.8±5.3
¹⁷⁰ Yb	990	990	0.0064	6.3±1.8
¹⁷⁶ Hf	685	701±91	0.0109	7.6±1.8
¹⁸³ W	260	260±30	0.0024	0.62±0.14
¹⁸³ W	550	550±50	0.005	0.28±0.06
¹⁸⁴ W	180	180±20	0.030	5.4±1.2
¹⁸⁶ Os	329	329	0.0113	3.7±1.1
¹⁸⁷ Os	873	873	0.0045	3.9±1.1
¹⁹² Pt	352	352	0.0099	3.5±1.0
¹⁹⁵ Hg	411	411	0.035	14±4
²⁰⁴ Pb	58.5	58±12	0.057	3.2±0.9
²⁰⁸ Pb	—	9.6±3.0	0.150	1.4±0.5
²⁰⁷ Pb	—	8.7±3.0	0.10	0.87±0.35

*Estimation of values of σ was carried out by the technique described in Ref. 48.

**The relative error in the values of N_g was taken as 20%. In those cases when σ is given without indication of the error, in evaluating σ/N_g the error in σ also is taken as 20%.

$$L^{-1} \frac{1}{((s/\lambda_k) + 1)^{m_k}}$$

best approximates

$$L^{-1} \prod_{i=1}^k \frac{1}{(s/\sigma_i) + 1}. \quad (13)$$

Here

$$\psi_k(\tau) = L^{-1} \bar{\psi}_k(s) = \frac{1}{2\pi i} \int_{-i\infty}^{i\infty} \exp(s\tau) \bar{\psi}_k(s) ds. \quad (14)$$

From this we obtain

$$\psi_k(\tau) \approx L^{-1} \frac{1}{[(s/\lambda_k)+1]^{m_k}} = \lambda_k \frac{(\lambda_k \tau)^{m_k-1}}{\Gamma(m_k)} \exp(-\lambda_k \tau). \quad (15)$$

Thus, the approximate CFHZ solution reduces to replacement of σ by λ_k , k by m_k , and $(k-1)!$ by $\Gamma(m_k)$, where

$$\lambda_k = \frac{s_1}{s_2}, \quad m_k = \frac{s_1^k}{s_2}, \quad (16)$$

$$s_1 = \sum_{i=1}^k \sigma_i^{-1}, \quad s_2 = \sum_{i=1}^k \sigma_i^{-1}.$$

As a control of the CFHZ solution we shall use the special case $\sigma_k = \alpha k$, where $\alpha = \text{const}$. In this case the Bateman expansion is easily summed and the exact solution is obtained in the form

$$\psi_k(\tau) = \sigma_k \exp(-\alpha\tau) [1 - \exp(-\alpha\tau)]^{k-1}. \quad (17)$$

For constant cross sections $\sigma_i = \sigma$ the CFHZ solution¹⁹ gives

$$\psi_k(\tau) = \sigma_k \frac{(\sigma\tau)^{k-1}}{(k-1)!} \exp(-\sigma\tau). \quad (18)$$

This function is analogous to a Poisson distribution in k . It reaches a maximum value at $k = \sigma\tau + 1$ which is equal to

$$\psi_k^{\text{max}} \approx \frac{\sigma_k}{\sqrt{2\pi\sigma\tau}}. \quad (19)$$

The distribution (18) has a width $\approx (2\pi\sigma\tau)^{1/2}$; its amplitude decreases and its width increases (expansion of the packet) with increase of σ and the neutron exposures τ . Although this investigation refers to constant capture cross sections, the expansion of the packet due to the random nature of the capture process is preserved also in the general case. It becomes more appreciable if the cross section increases with increase of k , for example, according to a law $\sigma_k = \alpha k$.

In Fig. 4a we have shown graphically the CFHZ general solution as a function of k and τ ($0 \leq k \leq 150$; 0.2

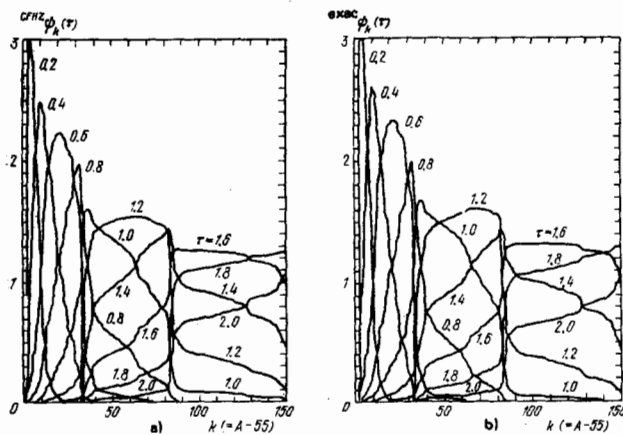


FIG. 4. a) Approximate solution of the CFHZ theory $\psi_k^{\text{CFHZ}}(\tau)$ as functions of k and τ .²¹ b) Exact solution of the Bateman equations $\psi_k^{\text{exact}}(\tau)$ as functions of k and τ .²¹ $\psi_k(\tau) = \sigma_k N_k(\tau)/N_1(0)$, where σ_k is the neutron-capture cross section, $N_k(\tau)$ is the yield of nuclei with mass number $A = k + 55$ in the s-process chain for a neutron exposure τ , and $N_1(0)$ is the number of seed nuclei at the initial moment of synthesis of elements in the s process.

$\leq \tau \leq 2$).

c) Exact solution

Recently Newman²¹ obtained an exact solution of the s-process equations on the basis of the Bateman expansion. This solution is shown in Fig. 4b for the same values of k and τ . As can be seen from Fig. 4, the CFHZ approximate solution is in good agreement with the exact solution for almost all values of $\psi_k(\tau)$ shown in these diagrams. At the same time a careful comparison reveals a difference of $\sim 10\%$ between the exact and approximate solutions even for large τ . This discrepancy is even more evident in Fig. 5, where the ratio of the exact solution to the CFHZ approximate solution is given. This figure shows a substantial difference between the exact and approximate solutions for small values of τ .

Let us discuss in more detail the features and difficulties of the exact numerical summation of the Bateman expansion (8). If this summation were carried out by a computer with unlimited accuracy, then it would be possible relatively easily to obtain solutions for all values of τ , including small values. For small τ , $\psi_k(\tau)$ decreases as τ^{k-1} . At the same time the products c_{ik} can be very large, since the cross sections σ_k cover a wide range of values from 8 to 3300 mb (see Table I). In this case a small value of $\psi_k(\tau)$ is obtained when the term with largest absolute value in the Bateman expansion is summed with many terms of the expansion which differ by several orders of magnitude but have different signs. Thus, the resulting error in a summation with finite accuracy of the calculations unavoidably turns out to be so large as to make these calculations no longer meaningful. This occurs when the number of orders of the ratio of the value of the maximum term in the expansion to the entire sum approaches the number of decimal digits of the computer. In Fig. 6 we have shown the ratio of the absolute value of the maximum term in the Bateman expansion to the value of the sum $\psi_k(\tau)$ as functions of k and τ .

It is evident from Fig. 6, for example, that $\psi_{150}(\tau=1.0)$

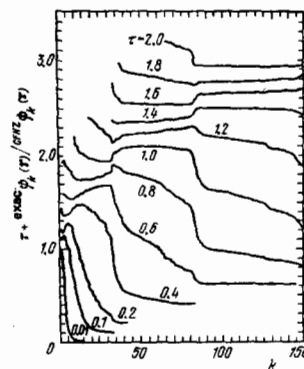


FIG. 5. Comparison of the exact solution of Bateman with the approximate CFHZ solution in the region of neutron exposures $0.01 \leq \tau \leq 2.0$ mb. The curves are cut off at small k when the ratio $\psi_k^{\text{exact}}(\tau)/\psi_k^{\text{CFHZ}}(\tau)$ exceeds 1.1 in order to avoid pileup. For the same reason in the axis of ordinates we have added τ to the ratio $\psi_k^{\text{exact}}/\psi_k^{\text{CFHZ}}$.

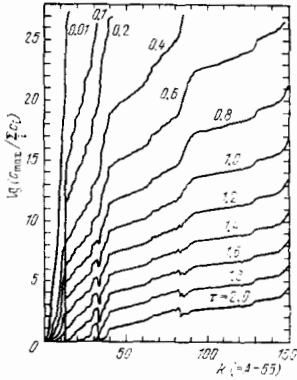


FIG. 6. Ratio of absolute value of the largest term in the Bateman expansion to the entire sum of the series, as functions of k and τ .²¹

requires at a least a calculational accuracy of 18 orders of magnitude. On the other hand $\psi_k(\tau=2.0)$ can be obtained for any k , using an accuracy of five orders of magnitude. Newman²¹ carried out calculations with an accuracy ≈ 27 orders of magnitude.

For small values of τ the difficulties in the calculations turn out to be especially great in the region $k < 30$. Unfortunately it is just in this region of τ and k that the CFHZ solutions become incorrect. Here, as can be seen from Fig. 7a, the $\psi_k(\tau)$ curves for $\tau < 0.7$ begin to drop rapidly with decreasing values of k , producing the difficulties described above. Therefore interest is presented by a different form of exact solution for small τ found by Newman²¹ which permits calculations of $\psi_k(\tau)$ to be carried out in this region:

$$\psi_k(\tau) = P_k(\tau) \sum_{n=0}^{\infty} A_{nk}(\tau), \quad (20a)$$

where

$$P_k(\tau) = \frac{\sigma_k \cdot \tau}{(k-1)!} P_{k-1}(\tau), \quad P_0(\tau) = \tau^{-1}, \quad (20b)$$

$$A_{nk}(\tau) = [(k-1)A_{n, k-1}(\tau) - \sigma_k \cdot \tau \cdot A_{n-1, k}(\tau)] \frac{1}{n+k-1} \quad (20c)$$

for $A_{0k}(\tau) = 1$ and $A_{n0}(\tau) = 0$. This form is convenient for programming and computations. Newman notes, however, that it is nevertheless difficult for calculations in the case of large τ , since it requires a large number

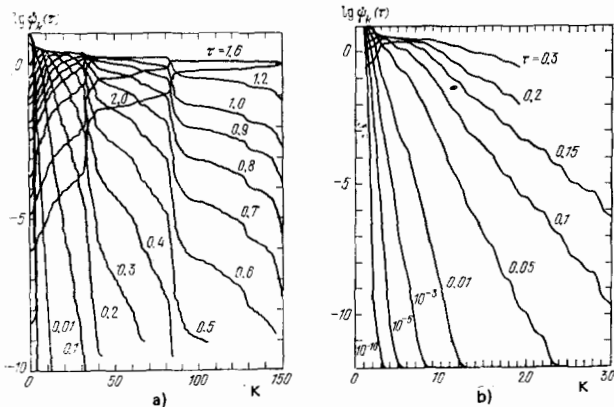


FIG. 7. a) Exact solution of the equations of Bateman²¹ on a semilogarithmic scale for $0.01 \leq \tau \leq 2$ mb; b) exact solution of the s -process equations proposed by Newman²¹ for small τ .

of terms in the expansion for convergence, while in the case of small τ the convergence is rather rapid.

In Fig. 7b we have shown the exact solution $\psi_k(\tau)$ with use of the Newman expansion in the region of small $\tau < 0.3$ where the CFHZ solution becomes unsuitable. This exact solution can be used directly for calculation of yields of elements with small values of neutron exposure, in particular for pulsed s processes where τ occurs in small batches ($10^{-3} - 10^{-1}$ mb⁻¹).^{22, 23}

In concluding a mathematical review of the exact theory of the s process we shall discuss cases of degeneracy in which the σ_k are so large that their logarithms are close together. In Eq. (9) the factors $(\sigma_j - \sigma_i)^{-1}$ are found by integration of $\exp[(\sigma_j - \sigma_i)\tau]d\tau$, and therefore when $\sigma_j = \sigma_i$ they become powers of τ . If there is an arbitrary number $n(k)$ of degenerate cross sections so that each σ_i has a degeneracy n_i , the solution for the Laplace transform will have the form

$$\bar{\psi}_k(s) = \prod_{i=1}^{n(k)} \left(\frac{\sigma_i}{\sigma_i + s} \right)^{n_i}. \quad (21)$$

In the inverse transformation we have

$$\psi_k(\tau) = \prod_{i=1}^{n(k)} \frac{\sigma_i^{n_i}}{(n_i-1)!} \frac{d^{n_i-1}}{ds^{n_i-1}} \left[\prod_{j=1}^{n(k)} \left(\frac{\sigma_j}{\sigma_j + s} \right)^{n_j} \exp(s\tau) \right]_{s=-\sigma_i} \quad (22)$$

with a pole of order n_i at $s = -\sigma_i$. As Clayton and Newman have shown,²⁴ in this case the expression for the function $\psi_k(\tau)$ in general form is found to be too cumbersome and unsuitable for calculation.

Newman used an artificial means of removing the degeneracy, which consisted of systematic multiplication of cross sections which were close in value by $1 + \delta\sigma$ ($\delta\sigma = 10^{-6}$) until the degeneracy was removed. This permits easy calculation of the yields of elements in the s process in the region of small τ .²¹

d) Comparison with experiment

Let us now consider the experimental data on neutron-capture cross sections in the light of the contemporary theory of the s process. Many of these cross sections have already been measured in laboratories,^{25, 26} but in most cases with not very high accuracy. At the same time a large number of neutron cross sections which are important for the theory of the s process remain unmeasured up to the present time. A further difficulty is the discrepancies in the experimental results, and also in many cases the unsatisfactory agreement with theory.

Recent calculations of Holmes²⁷ give a systematic estimate of the unmeasured neutron cross sections, but their accuracy is $\sim 200\%$. In 1976 Conrad²⁸ attempted to choose cross-section values which satisfy a smooth σN curve for the s process of the solar system. The main uncertainty in this choice is due to the uncertainty in taking into account the fraction of formation of the nuclides considered in the r process.

Newman²¹ gives his own set of recommended capture cross-section values. A complete summary of data on neutron cross sections, which includes values estimated by us and their error at the 68% confidence lev-

el, is given in Table I. All neutron cross-section values are given for the energy region $\sim 25-30$ keV. As will be shown below, the average thermodynamic conditions of the s process in the solar system correspond to just these thermal energies of the neutrons, i.e., to a temperature of the medium $\sim 3 \cdot 10^8$ K.

In the previous section we discussed various means of determining $\psi_s(\tau)$ as a function of the neutron exposure. Here the exact methods of solution confirmed the correctness of the CFHZ theory. Now for comparison of the theoretical values σN_s^{theo} and the values observed in the solar system σN_s^{exp} (where σ is the neutron-capture cross section and N_s^{exp} is the yield of a given nuclide in the s process), let us consider a set of values of various neutron exposures. Seeger, Fowler, and Clayton²⁹ and also Clayton and Ward³⁰ have shown that for a continuous exposure it is convenient to use the following expressions:

$$\sigma N_s^{\text{theo}} = \int_0^{\infty} \rho(\tau) \psi_s(\tau) d\tau, \quad (23)$$

$$\rho(\tau) = G \exp\left(-\frac{\tau}{\tau_0}\right); \quad (24)$$

here $\rho(\tau)d\tau$ is the number of seen nuclei of iron exposed to an integrated neutron flux τ in the interval $d\tau$; G and τ_0 are adjustable constants relating theory and experiment.⁶⁾

The curve in Fig. 8 was calculated with inclusion of Eqs. (23) and (24) for the constants $G \approx 1 \cdot 10^4$ ($\text{Si} \approx 10^6$) and $\tau_0 = 0.25 \text{ mb}^{-1}$.²² In this figure we have also shown the experimental values σN_s^{exp} and their total errors with inclusion of the cross-section values σ estimated by us, which are given in Table I. It should be noted that according to Ward and Newman²² the yields of most elements, except for the most volatile ones (Kr, Hg), have been measured rather well, with an accuracy $\sim 20\%$. Therefore we have taken the errors of all experimental yield values N_s^{exp} equal to 20% . As can be seen from the figure, very satisfactory agreement is observed between the s-process theory and the experimental values of σN_s^{exp} . However, in the region of nuclei close to iron an appreciable excess of the experimental values σN_s^{exp} over the theoretical curve is observed. In Ref. 22 this effect is explained as due to pulsation of the neutron flux.

e) The pulsed s process

The preceding analysis was carried out for thermodynamic conditions characteristic of the s process on the assumption of a constant temperature and density of the medium, which is subject to continuous neutron bombardment. However, as calculations have shown,³² the s process which is responsible for the yields of a

⁶⁾The results of a fit to the experimental σN_s values show that the observed distribution of $\sigma N_s(A)$ is best described by the sum of two exponentials in the expression for the neutron-exposure density $\rho(\tau)$: $\rho(\tau) = G_1 \exp(-\tau/\tau_{01}) + G_2 \exp(-\tau/\tau_{02})$. The physical reasons for the appearance of two values of the parameter τ_0 have been set forth by Ward *et al.*³³

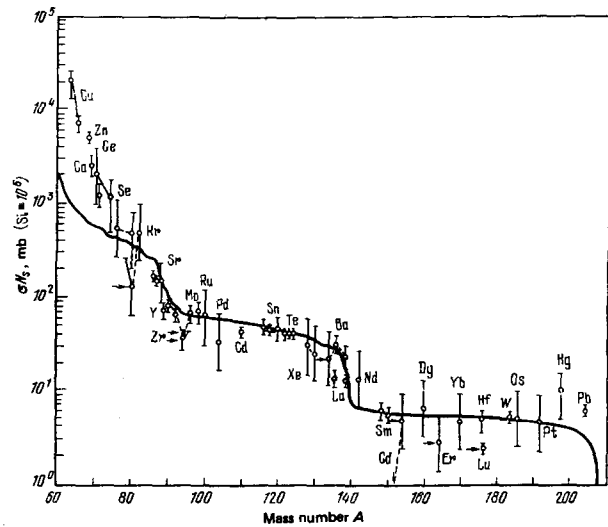


FIG. 8. Experimental curve $\sigma N_s = f(A)$ for the elements of the solar system. The arrows indicate nuclei which have been partially bypassed as the result of branching of the s process.

number of elements³¹ of the solar system occurs also in burning of the helium shell of stars of intermediate mass ($2-5 M_{\odot}$). In such processes the neutron flux obtained can have a pulsating nature^{22, 23} with short periods of neutron exposure (~ 10 years) separated by relatively long interpulse periods (~ 2500 years).

In discussing the pulsed s process an important role is played by periodic mixing of the matter when a flare of the helium shell puts matter rich in carbon in contact with matter enriched in hydrogen, leading to formation of seed nuclei and sources of free neutrons in accordance with the reaction $^{12}\text{C}(p, \gamma)^{13}\text{N}(\beta^+)^{13}\text{C}(\alpha, n)^{10}\text{O}$.

In Weigert's model of stellar mixing³⁹ the s process occurs as follows: 1) the neutron exposures are brief and occur periodically; here the quiet periods between flares are considerably longer than the periods of exposure; 2) the neutron exposure per flare is almost the same for the entire material contained in the convective zone (Fig. 9); 3) the convective zone loses mass at the time of the flare as the result of the fact that the rising jets transport material to the surface, and between flares as the result of the fact that part of the helium is converted into ^{12}C . If M_c is the mass of the convective shell, the value of which is approximately constant during the evolution of the star, then between successive flares there remains a portion of it αM_c . Those neutron-rich nuclei which leave the convective zone are effectively lost for the s process, since they are not in a position to capture neutrons; 4) at the beginning of each flare a mass $(1 - \alpha)M_c$ of material from the outer shell is carried into the convective zone. This material contains seed nuclei which have not previously been exposed to neutrons. In discussion of the pulsed s process the exponential form of the neutron exposure distribution function arises naturally. If α is the fraction of mass of the convective shell remaining between successive flares, then for the yield of matter ejected into the external shell we obtain

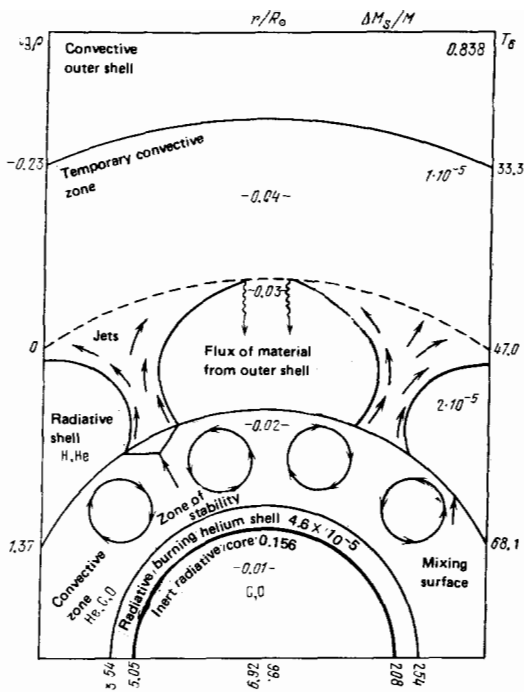


FIG. 9. Scheme of mixing of stellar matter in repeated flares of the helium shell.²³

$$\begin{array}{cccc} n & n+1 & n+2 & n+3 \\ 1-\alpha & (1-\alpha)\alpha & (1-\alpha)\alpha^2 & (1-\alpha)\alpha^3 \\ \Delta\tau & 2\Delta\tau & (3\Delta\tau) & 4\Delta\tau \end{array}$$

$$\rho(\tau) = \frac{1}{N_0} \frac{dN(\tau)}{d\tau} = \frac{1-\alpha}{\Delta\tau} \alpha^{\tau/\Delta\tau} = \Lambda \exp(-\Lambda\tau);$$

here N_0 is the initial number of seed nuclei in the external shell, Λ is an adjustable parameter chosen from the observed yields of elements in the solar system, and n is the number of the flare. In the pulsed s process the possibility arises for nuclei to decay between periods of neutron bombardment in the course of an interval $(3-4) \cdot 10^3$ years between flares. This decay can change the branching ratio if the neutron exposure during a flare is sufficiently small so that only a small quantity of unstable nuclei capture a neutron after being formed.

Analysis of the observed yields in several evolving stars (the stepped nature and the absence of clearly expressed peaks) shows that inside each star there is already created a superposition of different neutron exposures, i.e., the mechanism of the pulsed nature of the s process and the mixing of material inside a single star gives satisfactory agreement with observation.

Ulrich²³ showed that in the pulsed s process it is possible to synthesize all nuclei of the s process between $A=70$ and $A=205$ within a single star by means of repeated series of flares of its helium shell. For optimum parameters $1-\alpha=0.07$, $\Delta\tau=0.016$, $\Delta N_n=0.24$ (the number of captured neutrons in each heavy nucleus), approximately 80 flares are required to give the final distribution of the yields of the elements in the solar system. During each flare, for this set of parameters, about 5% of the mass between the hydrogen and helium shells is enriched in s -process elements and mixed with the outer shell of the star.

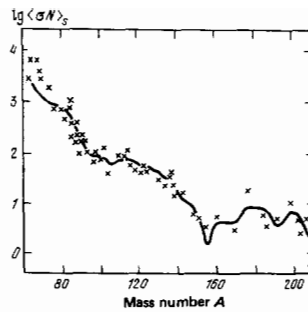


FIG. 10. Comparison of observed curve of yield of s -process elements with the calculations of Ulrich²³ (the figure is from Ref. 15).

For the unbranched s process, in the chain of which there are no long-lived nuclides ($T_{1/2} \lesssim 10$ years) and all β decays occur much more rapidly than neutron captures, we would not be able to distinguish pulsed and continuous neutron exposures. The main chain of the s process would not change in this case (see for example Fig. 3). The main consequence of pulsed bombardment is that as the result of intense neutron fluxes lasting ≈ 10 years, along the s -process chain there can be constructed also other nuclides than in the case of continuous neutron bombardment if there are long-lived nuclides at the branching points.

In Fig. 10 we have given a comparison of the yield curve calculated by Ulrich on the assumption of a pulsed neutron exposure and branchings of the s process. As can be seen from the figure, inclusion of a pulsed nature of the exposure and of branchings permits a better description of the structures in the steps between values of $\sigma N = \text{const}$.

3. BRANCHING OF THE s PROCESS

In nature there exist certain long-lived nuclei which in the track of the s process capture a neutron with a higher probability than that for β decay. As we have already mentioned above, this leads to branching of the s process. Generally speaking, each nucleus in the s -process chain is created and destroyed either by neutron captures or by nuclear transformations produced by weak interactions (β^+ decay, electron capture). When decay occurs too rapidly ($\lambda_\beta \gg \lambda_n$) or too slowly ($\lambda_\beta \ll \lambda_n$) relative to neutron capture, the nucleus under discussion can be removed from the chain or can be neglected. However, if competition exists between neutron capture and β decay, branching of the s process appears.

In Fig. 11 we have shown the track of a branched s process occurring through the isotopes of Kr, Rb, Sr, Y, and Zr. An example of branching is the fork in the region of ^{85}Kr . Here the main path of the s process is marked by the continuous line and the dashed line shows the possible branching (in particular, in the presence of pulsed neutron exposure as mentioned in the previous section). Following Ward *et al.*,³³ we introduce the notation $\lambda_n = n_n \langle \sigma v \rangle$, λ_- is the rate of β^- decay, λ_+ is the rate of β^+ decay, λ_{ec} is the rate of electron capture, and we shall consider the system of equations for the s

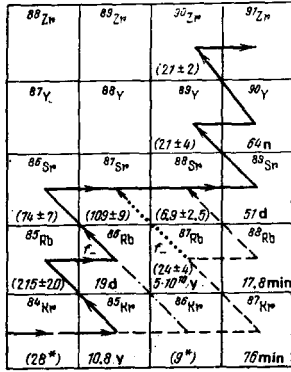


FIG. 11. Track of branched s process through the isotopes of Kr, Rb, Sr, Y, and Zr. The dashed line shows possible branchings from the main path of the s process.

process in the region of Kr, Rb, and Sr:

$$\begin{aligned}
 \frac{dN(^{86}\text{Kr})}{dt} &= \lambda_n(^{86}\text{Kr}) N(^{86}\text{Kr}) - [\lambda_-(^{86}\text{Kr}) + \lambda_n(^{86}\text{Kr})] N(^{86}\text{Kr}), \\
 \frac{dN(^{85}\text{Rb})}{dt} &= \lambda_-(^{85}\text{Rb}) N(^{85}\text{Rb}) - [\lambda_n(^{85}\text{Rb})] N(^{85}\text{Rb}), \\
 \frac{dN(^{86}\text{Kr})}{dt} &= \lambda_n(^{86}\text{Kr}) N(^{86}\text{Kr}) \\
 &\quad + [\lambda_{ec}(^{86}\text{Rb}) + \lambda_+(^{86}\text{Rb}) N(^{86}\text{Rb}) - \lambda_n(^{86}\text{Kr})] N(^{86}\text{Kr}), \\
 \frac{dN(^{86}\text{Rb})}{dt} &= \lambda_n(^{86}\text{Rb}) N(^{86}\text{Rb}) \\
 &\quad - [\lambda_-(^{86}\text{Rb}) + \lambda_{ec}(^{86}\text{Rb}) + \lambda_+(^{86}\text{Rb})] N(^{86}\text{Rb}), \\
 \frac{dN(^{86}\text{Sr})}{dt} &= \lambda_-(^{86}\text{Sr}) N(^{86}\text{Sr}) - \lambda_n(^{86}\text{Sr}) N(^{86}\text{Sr}), \\
 \frac{dN(^{87}\text{Rb})}{dt} &= \lambda_n(^{87}\text{Rb}) N(^{87}\text{Rb}) - [\lambda_n(^{87}\text{Rb}) + \lambda_-(^{87}\text{Rb})] N(^{87}\text{Rb})^7, \\
 \frac{dN(^{87}\text{Sr})}{dt} &= \lambda_n(^{87}\text{Sr}) N(^{87}\text{Sr}) + \lambda_-(^{87}\text{Rb}) N(^{87}\text{Rb}) - \lambda_n(^{87}\text{Sr}) N(^{87}\text{Sr}), \\
 \frac{dN(^{88}\text{Sr})}{dt} &= \lambda_n(^{88}\text{Sr}) N(^{88}\text{Sr}) + \lambda_n(^{87}\text{Rb}) N(^{87}\text{Rb}) - \lambda_n(^{88}\text{Kr}) N(^{88}\text{Kr}).
 \end{aligned}
 \tag{25}$$

In this system of equations the rates of electron capture and positron decay of ^{86}Rb have been included for generality of the picture, in order to illustrate the possibilities of multiple branching, although in fact $\lambda_-(^{86}\text{Rb}) \gg \lambda_{ec}(^{86}\text{Rb})$ or $\lambda_+(^{86}\text{Rb})$.

For solution of the system of equations (25) we can make a simplification related to the short half-life of ^{86}Rb :

$$0 = \lambda_n(^{86}\text{Rb}) N(^{86}\text{Rb}) - [\lambda_-(^{86}\text{Rb}) + \lambda_{ec}(^{86}\text{Rb}) + \lambda_+(^{86}\text{Rb})] N(^{86}\text{Rb}).
 \tag{26}$$

The differential equations (25) as before are solvable with difficulty, since in general form the density n_n and temperature T depend arbitrarily on the time. Therefore the next correct approximation is discussion of the s process for constant temperature T . As we have seen in section (b) of chapter 2, the CFHZ theory introduces the variable

$$\tau \equiv \int_0^t n_n(t') v_T dt',$$

which converts the main equation of the s process (1) to the form (4): $dN_A/d\tau = \sigma_{A-1} N_{A-1} - \sigma_A N_A$ without any assumptions regarding the dependence $n_n(t)$.

For a branched s process this simplification becomes

⁷As a result of the smallness of the half-lives, ^{87}Kr and ^{86}Rb are not preserved in the s-process chain: $\lambda_-(^{87}\text{Kr}) N(^{87}\text{Kr}) = \lambda_n(^{86}\text{Kr}) N(^{86}\text{Kr})$; $\lambda_-(^{86}\text{Rb}) N(^{86}\text{Rb}) = \lambda_n(^{87}\text{Rb}) N(^{87}\text{Rb})$.

impossible as a result of the fact that the rates of neutron capture in equations (25) depend on $n_n(t)$, while the rates of the weak interactions (electron capture and positron decay) do not depend on this quantity. Therefore the time t enters into the equations (25) as an independent variable and for arbitrary dependences $n_n(t)$ the equations can be solved by numerical integration.

However, if $n_n(t)$ is constant, then the set of equations (25) will contain constant coefficients and the system of first-order differential equations can be solved exactly. In this case Ward, Newman, and Clayton³³ again use the variable τ , which for constant n_n will be linearly proportional to the time.

Using the notation of section (b) of chapter 2, $\psi(A) = \sigma_A N(A)/N_0(^{56}\text{Fe})$, and introducing the quantity $f_- \equiv \lambda_- / (\lambda_- + \lambda_n + \lambda_{ec} + \lambda_+)$ which determines the branching of the β^- decay, we rewrite the system of equations (25) with inclusion of (26) in a form more convenient for analysis and computations:

$$\begin{aligned}
 \frac{d\psi(^{86}\text{Kr})}{d\tau} &= \sigma(^{86}\text{Kr}) \left[\psi(^{86}\text{Kr}) - \frac{1}{1-f_-(^{86}\text{Kr})} \psi(^{86}\text{Kr}) \right], \\
 \frac{d\psi(^{85}\text{Rb})}{d\tau} &= \sigma(^{85}\text{Rb}) \left[\frac{f_-(^{86}\text{Kr})}{1-f_-(^{86}\text{Kr})} \psi(^{86}\text{Kr}) - \psi(^{85}\text{Rb}) \right], \\
 \frac{d\psi(^{86}\text{Kr})}{d\tau} &= \sigma(^{86}\text{Kr}) \{ \psi(^{86}\text{Kr}) + [1-f_-(^{86}\text{Rb})] \psi(^{86}\text{Rb}) - \psi(^{86}\text{Kr}) \}, \\
 \frac{d\psi(^{86}\text{Sr})}{d\tau} &= \sigma(^{86}\text{Sr}) [f_-(^{86}\text{Rb}) \psi(^{86}\text{Rb}) - \psi(^{86}\text{Sr})], \\
 \frac{d\psi(^{87}\text{Rb})}{d\tau} &= \sigma(^{87}\text{Rb}) \left[\psi(^{86}\text{Kr}) - \frac{1}{1-f_-(^{87}\text{Rb})} \psi(^{87}\text{Rb}) \right], \\
 \frac{d\psi(^{87}\text{Sr})}{d\tau} &= \sigma(^{87}\text{Sr}) \left[\psi(^{86}\text{Sr}) + \frac{f_-(^{87}\text{Rb})}{1-f_-(^{87}\text{Rb})} \psi(^{87}\text{Rb}) - \psi(^{87}\text{Sr}) \right], \\
 \frac{d\psi(^{88}\text{Sr})}{d\tau} &= \sigma(^{88}\text{Sr}) [\psi(^{87}\text{Rb}) + \psi(^{87}\text{Sr}) - \psi(^{88}\text{Sr})].
 \end{aligned}
 \tag{27}$$

The quantity f_- depends on the density n_n and temperature T and also on the electron density n_e (in the presence of sufficiently intense electron capture).

Since all these parameters depend on time, the coefficients of the equations (27), generally speaking, also depend on τ . For constant n_n and constant thermal environment (a special case) f_- and the coefficients of the equations (27) are constant quantities. Physically the pattern of neutron bombardment in this case can be represented by an extended rectangular pulse with steep fronts. In a comparison with observational yields of nuclides in the s process this means that $n_n(t)$ falls off so rapidly that the yields of nuclides essentially do not change for a rapid change of $n_n(t)$.

The classical theory of the s process assumes $f_- = 1$ for all decaying nuclei. Therefore the model of Ward, Newman, and Clayton, which considers the value $f_- < 1$, is a generalization of the traditional picture of the s process, disregarding the assumption $f_- = \text{const}$. In addition, some f_- values depend on T and with allowance for this dependence it is possible to calculate more accurately the yields in the theory of the s process.

Omitting the mathematical operations in the model considered,³³ for the yields of each of seven nuclei of the branch lying beyond ^{84}Kr – ^{85}Kr , ^{86}Kr , ^{85}Rb , ^{87}Rb , ^{86}Sr , ^{87}Sr , and ^{88}Sr —we shall write the exact solution in the form

$$\psi_i(\tau) = \sigma(^{86}\text{Kr}) \sum_{j=1}^7 A_{ij} \exp(\beta_j \tau) \int_0^\tau \exp(-\beta_j \tau') \psi(^{86}\text{Kr}, \tau') d\tau'; \tag{28}$$

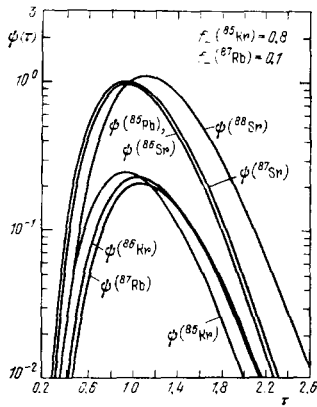


FIG. 12. The dependence $\psi(A)$ for nuclei of the ^{85}Kr branch for different values of the branching ratio f_- .³³

here β_i and A_i are the coefficients of the expansion (the cross sections or combinations of cross sections and branching ratios f_- for the seven nuclides considered).

This expression, for each of the seven nuclei of the branch determines the quantity $\psi_i(\tau)$ as a function of ψ for the nucleus with which the branch begins (in this case ^{84}Kr) and as a function of the cross sections and branching ratios. In order to calculate ψ_i it is necessary to know the functional dependence of the seed term $\psi(^{84}\text{Kr})$. In Figs. 12 and 13 we have given the results³³ for various terms of the ^{85}Kr branch calculated with characteristic values of $f_-(^{85}\text{Kr})$ and $f_-(^{87}\text{Rb})$. As can be seen from Fig. 13, the results of calculation of $\psi(\tau)$ with inclusion of branching ($f \neq 1$) differ from the values of $\psi(\tau)$ obtained in the absence of branching (the canonical path).

Ward *et al.*³³ have discussed a numerical example of the effect of the ^{79}Se and ^{85}Kr branches on the value of $\psi(^{90}\text{Zr})$. The function $\psi^0(^{90}\text{Zr})$ (the unbranched s process) is calculated on the assumption that ^{79}Se always captures a neutron and ^{85}Kr always undergoes β^- decay ($f_- = 1$). The function $\psi^{\text{bran}}(^{90}\text{Zr})$ is calculated with allowance for previous branchings with $f_-(^{79}\text{Se}) = 0.2$ and

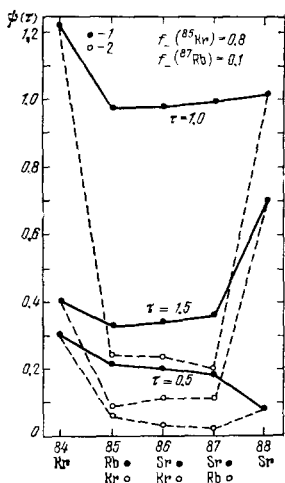


FIG. 13. The dependence $\psi(A)$ for nuclei of the ^{85}Kr branch for various values of τ .³³ 1—Canonical path, 2—path with inclusion of branching.

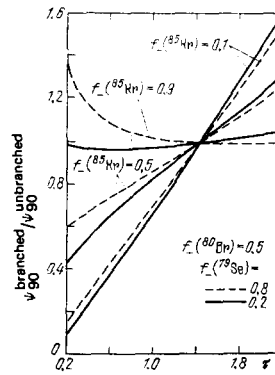


FIG. 14. Effect of s-process branchings at ^{79}Se and ^{85}Kr on the value of $\psi(^{90}\text{Zr})$.³³

0.8 and $f_-(^{85}\text{Kr}) = 0.1, 0.5, \text{ and } 0.9$.

We have shown the results of these calculations in Figs. 14 and 15. Figure 14 shows the ratio $\psi_{90}^{\text{bran}}/\psi_{90}^0$ as a function of τ for various values of $f_-(^{85}\text{Kr})$ and for two different values of $f_-(^{79}\text{Se})$. As can be seen from this figure, the quantity $f_-(^{85}\text{Kr})$ has a strong influence on the yield $\psi(^{90}\text{Zr})$ in the s process. Physically this means that the s process through ^{86}Kr is delayed by the small capture cross sections of ^{86}Kr and ^{87}Rb with respect to the s process through ^{86}Sr and ^{87}Sr (see Fig. 11). If f_- is close to unity, then the yield of ^{90}Zr in the s process is completely determined by the canonical path through ^{86}Sr and $\psi_{90}^{\text{bran}} \approx \psi_{90}^0$. On the other hand, if f_- is small, then for small exposures τ the yield of ^{90}Zr is determined by the branching through ^{86}Kr and ^{87}Rb , for which small capture cross sections are characteristic, and $\psi_{90}^{\text{bran}} < \psi_{90}^0$. For large neutron exposures τ and small f_- , even in spite of the small σ of ^{86}Kr and ^{87}Rb , ψ_{90}^{bran} becomes greater than ψ_{90}^0 .

In Fig. 15 we have shown directly the ratio $\psi_{90}^{\text{bran}}/\psi_{90}^0$ as a function of $f_-(^{85}\text{Kr})$ for the chosen values of τ . Both these plots therefore show that the influence of branching on the yields of nuclei in the s process can be substantial.

For comparison of the theoretical yields ψ_A with the curve of σN in the solar system it is necessary, as we have already noted above, to consider the superposition of neutron exposures τ . Here one usually considers an

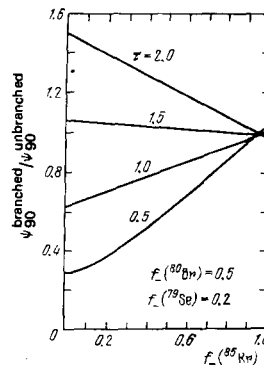


FIG. 15. The ratio $\psi(^{90}\text{Zr})/\psi_0(^{90}\text{Zr})$ as a function of $f_-(^{85}\text{Kr})$ for characteristic values of neutron exposure.

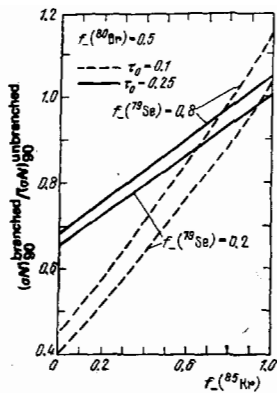


FIG. 16. Effect of s-process branchings on the value of $\psi(^{90}\text{Zr})$ for an integrated neutron exposure.³³

exponential distribution of exposures $\rho(\tau) = G \exp(-\tau/\tau_0)$, where $\tau_0 = 0.25 \text{ mb}^{-1}$ and $G = 10^4$ ($\text{Si} = 10^6$).

In Fig. 16 we have shown the same effect as in Fig. 15 but integrated over $\rho(\tau)$ for $\tau_0 = 0.25$ and 0.1 mb^{-1} . As can be seen from the figure, the effect of branching at ^{85}Kr on the yield in the s process of ^{90}Zr as a function of the value of $f_-(^{85}\text{Kr})$ is retained also for superpositions of different neutron exposures.

The effect of a relative "hindrance" of the s process at small neutron cross sections can be illustrated in the case of a simple branching of very fast β^+ decays³³ (Fig. 17). For any nucleus formed beyond this branch the ratio of the σN values along the branches σ_2 and σ_1 will be determined by the simple expression⁸⁾

$$R = \frac{\sigma_2(1 + \tau_0\sigma_1)}{\sigma_1(1 + \tau_0\sigma_2)}. \quad (29)$$

In Fig. 17 σ_1 is fixed and equal to 100 mb. The effect of a relative hindrance of the s process through the branch σ_2 on the yields of nuclides in the solar system turns out to be very substantial for $\sigma_2 \ll \sigma_1$.

In Fig. 18 we have shown how the branchings at ^{79}Se and ^{85}Kr affect the calculated σN curve normalized to $(\sigma N)_{^{74}\text{Ge}} = 1$. The canonical yields of nuclei in the s

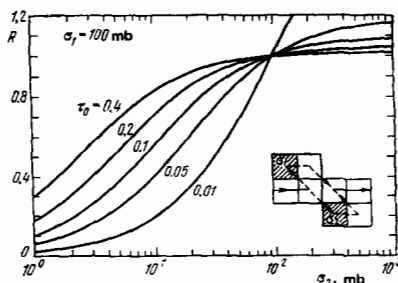


FIG. 17. Effect of a relative "hindrance" of the s process for small neutron cross sections.³³

⁸⁾This is seen most easily if one uses the simple form of σN_A^{theo} proposed in Ref. 30:

$$\sigma N_A^{\text{theo}} = G \sum_{i=56}^A \left(1 + \frac{1}{\tau_0\sigma_i}\right)^{-1}. \quad (30)$$

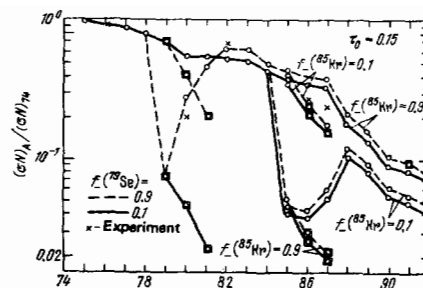


FIG. 18. Effect of branching at ^{79}Se and ^{85}Kr on the behavior of the $(\sigma N)_A$ curve.³³ The circles represent the yields of nuclei in the s process without allowance for branchings at ^{79}Se and ^{85}Kr , and the squares represent the yields of nuclei with allowance for these branchings. The experimental values are shown by crosses.

process are represented by the circles, and the yields of nuclei with allowance for branching are shown by the squares. The experimental values are given by the crosses.

4. THERMODYNAMIC CONDITIONS OF THE s PROCESS

Using the formalism developed above,³³ we can evaluate the average thermodynamic conditions of the s process on the basis of comparison of the synthesis of heavy elements in several key branchings of the s process. Considering all branchings as a function of the average thermodynamic conditions, for any two nuclei along the s-process track we have

$$\frac{\lambda_n^i}{\lambda_n^j} = \frac{\sigma_i}{\sigma_j}, \quad (31)$$

$$\frac{i^j(T)}{i^i(T)} = \left\{ \left[\frac{1}{f_i^j(T, n_e)} - 1 \right] \left[\frac{1}{f_j^i(T, n_e)} - 1 \right]^{-1} \right\} \frac{\sigma_i(T)}{\sigma_j(T)}, \quad (32)$$

where t_+ is the half-life for β^+ decay.

The ratios of the branchings $f^i(T, n_e)$ are determined by fitting the observed σN ratios within each branch and are functions of the temperature and the free electron density n_e .

If the cross sections, yields, and β -decay rates are well known, then for all possible combinations of branchings we can obtain from the equations (32) a set of permissible values of T and n_e (and consequently of the neutron density n_n) and choose from it consistent values of the average temperature and neutron density in the s process. Ward, Newman, and Clayton chose as a normalizing branch the ^{85}Kr branch, which does not contain internal branchings. Of course, it is difficult to expect that this procedure will lead to accurately agreeing values of T and n_e for different s-process nuclides, but it permits establishment of reasonable limits on the thermodynamic conditions of the s process.

Thus, the average temperature and the electron density at which synthesis of the i -th nuclide occurs are calculated from relations of the type

$$\frac{i^j(T)}{i^i(T)} = \left(\frac{f_j}{f_i} \right)_{^{85}\text{Kr}} \left[\frac{1 - f_i(T, n_e)}{f_i(T, n_e) \sigma} \right]_i. \quad (33)$$

In this relation the temperature dependence of the parameters is determined not only by the dependence

of the rate of β decay on temperature, but also by the possible temperature dependence of the quantity $\sigma\tau_0$, where τ_0 is the adjustable parameter in the expression for the neutron-exposure distribution density. However, as Clayton³⁴ showed, $\tau_0(kT) \approx (kT/30 \text{ keV})^{0.7} \tau_0(30 \text{ keV})$, and since in most cases $\sigma \propto T^{-1/2}$, then we have $\sigma\tau_0 \propto T^{0.2}$. This temperature dependence turns out to be much weaker than the temperature dependence of the β -decay rate.

The dependence of the rate of β decay on the temperature was calculated in 1973 by Newman.³⁵ The main effects which were considered here are the influence of excited states of the nucleus³⁶ and of electron capture in a vacancy of the atom.^{37,38} Figure 19 gives the main temperature dependence of the half-life $t_{1/2}$ for β^- emitters along the branched track of the s process. In Fig. 20 the substantial influence of temperature and electron density on the behavior of the multiple branching at ^{64}Cu is demonstrated. Variation of T and n_e leads to significant deviations of $f_{-}(^{64}\text{Cu})$ from the laboratory value 0.38. Finally, with allowance for the dependence $\sigma \propto T^{-1/2}$ mentioned above, the average neutron density n_n and the average neutron flux Φ are given by the relations

$$n_n = \frac{\ln 2}{v_T \sigma t_n} = \frac{9.15 \cdot 10^{10}}{\sigma t_n} \text{ cm}^{-3}, \quad (34)$$

$$\Phi = v_T n_n = \frac{1.18 \cdot 10^{10} \sqrt{T_8}}{\sigma t_n} \text{ cm}^{-2} \text{ sec}^{-1}. \quad (35)$$

Here $T_8 = 10^{-8} T \text{ K}$, $t_n = \ln 2 / \lambda_n$ is the "half-life"⁹⁾ against neutron capture (in years), and $\sigma(30 \text{ keV})$ is in millibarns.

Ward, Newman, and Clayton³³ on the assumption of an average density of the burning helium shells $\rho = 2000 \text{ g/cm}^3$ (Refs. 39, 40, and 32) calculated several key branchings of the s process, using them as indicators of the average temperature and time scale of the s process. The results of their calculations are given in Table II. As can be seen from this table, the average temperature of the s process is found to be $\sim 3 \cdot 10^8 \text{ K}$.

In the first column of the table for each nuclide which provides branching we have given the values of the neu-

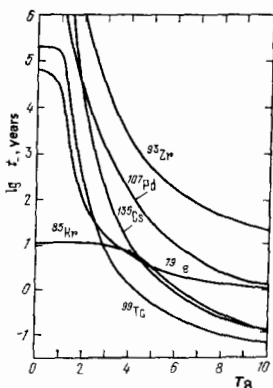


FIG. 19. Temperature dependence of the half-lives $t_{1/2}$ for "key" nuclei of the branched s process.

⁹⁾ The lifetime of this nucleus with respect to neutron capture is $t_n = \ln 2 / \lambda_n$.

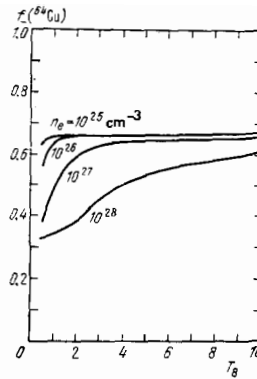


FIG. 20. Temperature dependence of the quantity $f_{-}(^{64}\text{Cu})$ for various values of electron density.

tron-capture cross sections, in the second column—the half-life measured in the laboratory, in the third column—the calculated branching ratios, in the fourth column—the temperature T_8 necessary for agreement with the branching at ^{85}Kr , in the fifth column—the half-life against β decay at a temperature T_8 , and finally in the sixth column—the resulting "half-life" t_n against neutron capture.

In spite of the fact that the analysis of Ref. 33 depends on estimated values of the neutron cross sections and β -decay properties of the excited states of the nuclei, for the average thermodynamic conditions of the medium in which the s process occurs a satisfactorily consistent picture is obtained if we take $T_8 = 3.1$, $n_n = 1.6 \cdot 10^7 \text{ cm}^{-3}$ ($\rho = 2000 \text{ g/cm}^3$), and $\Phi \approx 3.5 \cdot 10^{15} \text{ cm}^{-2} \text{ sec}^{-1}$. These values are comparable with the recent theoretical results: $T_8 = 2.5$ and $\Phi = 6.3 \cdot 10^{16} \text{ cm}^{-2} \text{ sec}^{-1}$.⁴² Ulrich, using the model of pulsed neutron exposure [see section (e) of chapter 2] obtains good agreement in the yields of nuclides produced through the ^{79}Se and ^{85}Kr branches, using the following values of flux and temperature at the time of the neutron flares: $\Phi = 4 \cdot 10^{16} \text{ cm}^{-2} \text{ sec}^{-1}$, $T_8 = 2.5$. These ranges of temperatures ($T_8 = 1-4$)^{43,44} and neutron fluxes ($\Phi = 10^{15} - 10^{16} \text{ cm}^{-2} \text{ sec}^{-1}$) can arise in the reactions $^{13}\text{C}(\alpha, n)^{16}\text{O}$, $^{17}\text{O}(\alpha, n)^{20}\text{Ne}$, and $^{20}\text{Ne}(\alpha, n)^{25}\text{Mg}$ in burning helium shells of highly evolved stars. In Table III we give the results of calculations of other s-process branchings on assumption of the average temperature and neutron-density values calculated above: $T_8 = 3.1$, $n_n = 1.6 \cdot 10^7 \text{ cm}^{-3}$.

In concluding this section, let us consider in accor-

TABLE II.

Branching nuclides	σ , mb	t_{β} (lab), years	f_{β}	T_8	$t_{\beta}(T_8)$, years	$t_n(T_8)$, years
^{79}Se	250	$6.5 \cdot 10^4$	0.58	2.9	17	23
^{80}Br	—	$3.4 \cdot 10^{-5}$	0.46	2.9	—	—
^{85}Kr	125	1.1 · 10	0.82	~3	~10	~46
^{95}Zr	70	$9.5 \cdot 10^6$	0.28	?	?	—
^{107}Pd	840	$9.0 \cdot 10^{15}$	0.032	3.3	190	6.3
^{113}Cd	1000	2.1	0.72	3.4	2.1	5.3
^{135}Cs	2500	9.3 · 10	0.076	?	< 93	< 7.6
^{151}Sm	—	$1.3 \cdot 10$	0.97	> 2	< 0.016	—
^{163}Dy	4640	8.6	0.83	?	< 8.6	< 42
^{169}Ho	1800	∞	0.29	~4	~6.3	~2.6
^{178}Lu	2820	3.3 · 10	0.23	~4	~5.1	~1.5
	2250	$2.6 \cdot 10^{10}$	0.67	?	—	—

TABLE III.

Branching nuclides	σ , mb	t_p (lab), years	t_p	t_p (T_{90}), years	t_n (T_{90}), years
^{63}Ni	30	$1.0 \cdot 10^8$	0.66	100	190
^{64}Cu	—	$1.5 \cdot 10^8$	0.64	—	—
^{81}Kr	450	$2.1 \cdot 10^8$	0.51	12	13
^{99}Tc	800	$2.1 \cdot 10^8$	0.56	5.6	7.2
^{107}Pd	950	$6.5 \cdot 10^8$	0.0066	910	6.0
^{132}I	450	$1.6 \cdot 10^7$	0.96	0.55	13
^{134}Cs	200	$2.3 \cdot 10^6$	0.29	71	29
^{147}Pm	1100	2.6	0.67	2.6	5.2
^{152}Gd	2500	0.66	0.78	0.63	2.3
^{154}Eu	1700	4.8	0.41	4.8	3.4
^{160}Tb	4100	0.20	0.87	0.20	1.4
^{170}Tm	3200	0.35	0.84	0.35	1.8
^{171}Tm	1300	1.9	0.70	1.9	4.4
^{189}Ta	2300	0.32	0.89	0.32	2.5
^{193}Ir	2100	0.20	0.93	0.20	2.7
^{192}Pt	1100	50	0.031	160	5.2
^{204}Tl	134	3.8	0.92	3.8	43
^{204}Pb	54	$1.4 \cdot 10^7$	0.45	130	105

dance with Ref. 33 the average time $\langle t \rangle$ of the s process which is found for a constant neutron flux Φ :

$$\langle t \rangle = \left[\Phi \int_0^\infty \rho(\tau) \frac{dn_s(\tau)}{d\tau} d\tau \left(\int_0^\infty \rho(\tau) n_s(\tau) d\tau \right)^{-1} \right]^{-1} = \frac{\tau_0}{\Phi}; \quad (36)$$

here $\rho(\tau)$ as before is an exponential: $\rho(\tau) = G \exp(-\tau/\tau_0)$; $n_s(\rho)$ is the number of neutron captures per seed nucleus.¹⁰⁾

From Eq. (36) for the values $\tau_0 = 0.25 \text{ mb}^{-1}$ and $\Phi = 3.5 \cdot 10^{15} \text{ cm}^{-2} \text{ sec}^{-1}$ we obtain

$$\langle t \rangle = 2270 \text{ years},$$

i.e., for production of the heavy elements of the s process at least several thousand years of neutron bombardment is required to obtain the observed distribution.¹¹⁾

5. CHRONOLOGY OF THE s PROCESS

To determine the age of nuclei formed in the s process of nucleosynthesis, Audouze, Fowler, and Schramm⁵² proposed to use the long-lived nuclide ^{176}Lu , which apparently is produced only in the s process. Lutecium 176 is screened from the r process by the

¹⁰⁾The average number of neutron captures per exposed seed nucleus is given by the expression

$$N_c = \int_0^\infty \rho(\tau) n_s(\tau) d\tau \left(\int_0^\infty \rho(\tau) d\tau \right)^{-1}$$

and, as can be shown, for $\tau_0 = 0.25$ we have $N_c = 4.8$. This corresponds to $8.5 \cdot 10^3$ captured neutrons (on the scale $\text{SI} = 10^6$).

¹¹⁾Burbidge *et al.*⁹ defined two types of branching of slow neutron capture in the case of ^{79}Kr and ^{151}Sm , which can serve as a characteristic of the time scale of the s process if the β decay lifetimes of the nuclides of these branches are used. Accordingly two different values are obtained for the time between successive neutron captures (10^5 years for nuclei with $A < 100$ and ten years for $A > 100$). However if one takes into account the dependence of the β -decay lifetimes on temperature and also the pulsed nature of the neutron exposure, the branch at ^{151}Sm is consistent with the same conditions and time scales which are necessary for all other branches of the s process. The large yields of nuclides with $A \geq 100$, which Burbidge *et al.*⁹ explained by a higher neutron flux, now are assigned to irradiation by the same neutron flux (as for $A < 100$) but for a longer time (continuously or in flares).¹⁵

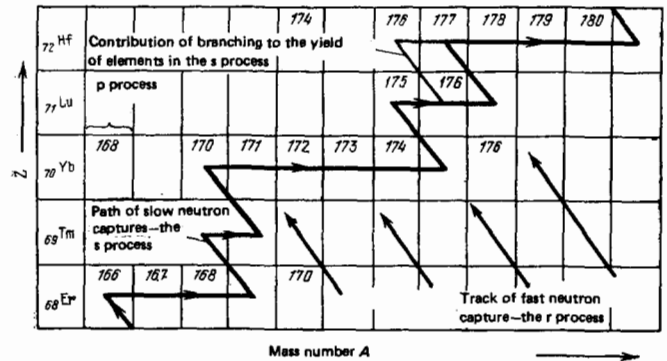


FIG. 21. Formation of isotopes of lutecium, ytterbium, and hafnium in the s process.

ytterbium isotope ^{176}Yb . The contribution of the p process¹²⁾ to the yield of ^{176}Lu can be estimated from the yields of the odd-odd nuclei ^{138}La and ^{180}Ta , which are produced in the p process. Such an estimate shows that the component of the p process in formation of ^{176}Lu is less than 5% (Fig. 21).

The half-life of ^{176}Lu has been measured repeatedly and highly divergent results have been obtained, from $2.1 \cdot 10^{10}$ to $7.3 \cdot 10^{10}$ years. However, the values of $T_{1/2}(^{176}\text{Lu})$ published during the last fifteen years are grouped roughly in the region $(3.6-4.0) \cdot 10^{10}$ years. In particular, in 1980 a careful measurement by Norman gives the value $(4.08 \pm 0.24) \cdot 10^{10}$ years. We shall adopt here an average value estimated from the results of five recent studies: $T_{1/2}(^{176}\text{Lu}) = (4.0 \pm 0.3) \cdot 10^{10}$ years.

The yield of a long-lived radioactive nuclide with atomic weight A (in the model of continuous synthesis) is determined by the relation

$$N_A(t_p) = \exp[-\lambda_A(\theta_{ss} + \Delta)] \int_0^{\Delta} a_A(t) \exp(\lambda_A t) dt; \quad (37)$$

here λ_A is the decay constant, θ_{ss} is the age of the solar system, Δ is the duration of nucleosynthesis prior to formation of the solar system, a_A is the rate of production of given nuclide in the nucleosynthesis process, and t_p is the present point of time. In the case of uniform synthesis [$a_A(t) = \text{const}$] we obtain

$$N_A(t_p) = \frac{a_A}{\lambda_A} \exp[-\lambda_A(\theta_{ss} + \Delta)] [\exp(\lambda_A \Delta) - 1]; \quad (38)$$

For a stable nucleus with atomic weight A' we have $N_{A'}(t_p) = a_{A'}^{st} \Delta$. Choosing the stable isotope of lutecium ^{175}Lu as a standard for calculation of the relative yield of ^{176}Lu , we have

$$\frac{N(^{176}\text{Lu})}{N_s(^{175}\text{Lu})} = \frac{a_{176}}{a_{175}} \frac{\exp[-\lambda_{176}(\theta_{ss} + \Delta)]}{\Delta \lambda_{176}} [\exp(\lambda_{176} \Delta) - 1]; \quad (39)$$

here N_s is the yield of ^{175}Lu resulting from the s process,¹³⁾ and Δ_s is the duration of the s process of nucle-

¹²⁾The p process is the absorption of protons in a (p, γ) reaction leading to appearance of certain heavy proton-rich nuclides which cannot be formed in neutron capture.

¹³⁾The main contribution to formation of ^{175}Lu (90%) is from the r process; $N_s(^{175}\text{Lu}) = N(^{175}\text{Lu}) - N_r(^{175}\text{Lu})$. See Table IV.

osynthesis before formation of the solar system.¹⁴⁾ The quantity $\theta_{ss} + \Delta$ is the age of the nuclides formed in the s process. Thus, if the yields $N(^{176}\text{Lu})$ and $N_s(^{175}\text{Lu})$ and the ratio of their rates of production are known, then Eq. (39) permits determination of the age of the s-process nuclides. The quantity a_{176}/a_{175} has not been established at the present time, but it can be estimated using the main conclusion of s-process theory that the rates of production of nuclei close in A are inversely proportional to their neutron-capture cross sections:

$$\frac{a_{176}}{a_{175}} = \frac{\sigma_{175}}{\sigma_{176}}. \quad (39a)$$

However, it is necessary here to take into account that ^{176}Lu in addition to the ground state, which decays to ^{176}Hf with a decay constant $\lambda_{176} = 1.73 \cdot 10^{-11} \text{ y}^{-1}$, has a 290-keV isomeric state which also decays to ^{176}Hf but with a short half-life of 3.7 hours. Consequently in the s process only a fraction of the neutron capture $^{175}\text{Lu} + n$ will go to the long-lived state of ^{176}Lu .⁵² This branching fraction

$$B = \frac{\sigma[^{175}\text{Lu}(n, \gamma)^{176}\text{Lu}]}{\sigma[^{175}\text{Lu}(n, \gamma)^{176}\text{Lu} + ^{176m}\text{Lu}]} \quad (39b)$$

has not been measured for neutron energies ~ 30 keV. The best estimate of B at thermal energies⁵² is $B = 0.22 \pm 0.17$. McCulloch, Laeter, and Rosman,⁵⁵ assuming that $N_s \sigma$ in the region of mass numbers $145 \leq A \leq 200$ amounts to 6.0, obtained $0.35 \leq B \leq 0.42$. Thus, the spread in the possible values of B covers the region from 0.2 to 0.4. With allowance for the branching ratio B , Eq. (39a) goes over to (39c):

$$\frac{a_{176}}{a_{175}} = B \frac{\sigma_{175}}{\sigma_{176}}. \quad (39c)$$

In addition to the uncertainty of the value of B , for the lutecium isotopes up to the present time there are no reliable data on the neutron capture cross sections and, what is most important, it is difficult to estimate the fraction of lutecium 175 produced only in the s process. Preliminary estimates on the basis of Eq. (39) show that the value of Δ_s is comparable in order of magnitude with the duration of nucleosynthesis calculated on the basis of other radioactive chronometers ($^{238}\text{U}/^{232}\text{Th}$, $^{187}\text{Re}/^{187}\text{Os}$).⁵⁴

Equation (39) is not very sensitive to variation of the quantity Δ_s . For calculation of the duration of the s process of nucleosynthesis in the Galaxy it is possible to use instead of $^{176}\text{Lu}/^{175}\text{Lu}$ another pair of nuclides: $^{176}\text{Lu}/^{176}\text{Hf}$.¹⁵⁾ Hafnium 176 is a stable daughter nucleus of lutecium 176 and is produced only in the s process.

According to Schramm and Wasserburg⁵⁶

$$\Delta_s = \frac{1}{\lambda_{176}} \ln \left[\frac{a(^{176}\text{Lu})}{a(^{176}\text{Hf})} \frac{N(^{176}\text{Hf})}{N(^{176}\text{Lu})} \right]; \quad (40)$$

here $N(^{176}\text{Hf})$ and $N(^{176}\text{Lu})$ are the yields of ^{176}Hf and ^{176}Lu at the moment of formation of the solar system.

¹⁴⁾ Δ_s is the time during which the s-process products observed today in the solar system were synthesized in the Galaxy in stars of the first generation.

¹⁵⁾ As nuclides close in A in a pair with ^{176}Lu it is possible to use also the stable nuclides ^{170}Yb and ^{182}W .^{52, 55}

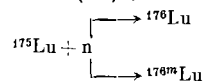
TABLE IV.

Nuclide	Process	Yield (Si $\approx 10^6$)	Cross section σ , mb	Yield in s process	Yield in r process
^{175}Lu	s, r	0.0334	1460 ± 110	0.00414	0.02929
^{176}Lu	s	0.00097	2250 ± 200	0.00097	—
^{176}Hf	s	0.0079	700 ± 90	0.0079	—

Using the approximation $\sigma(^{176}\text{Lu}) \cdot a(^{176}\text{Lu}) \approx \sigma(^{176}\text{Hf}) \cdot a(^{176}\text{Hf})$, we obtain

$$\Delta_s = \frac{1}{\lambda_{176}} \ln \left[\frac{\sigma(^{176}\text{Hf})}{\sigma(^{176}\text{Lu})} \frac{N(^{176}\text{Hf})}{N(^{176}\text{Lu})} \right]. \quad (41)$$

Equation (41) with allowance for the branching



goes over into (42):

$$\Delta_s = \frac{1}{1.73 \cdot 10^{-11}} \ln \left[\frac{B \sigma(^{176}\text{Hf})}{(1-B) \sigma(^{176}\text{Lu})} \frac{N(^{176}\text{Hf})}{N(^{176}\text{Lu})} \right]. \quad (42)$$

The quantities entering into Eq. (42) are given in Table IV.

If we adopt a value of the branching fraction $B \geq 0.3$, Eq. (42) gives the following estimate of the duration of the s process of nucleosynthesis in the Galaxy: $\Delta_s \approx 5 \cdot 10^9$ years. Consequently the age of the elements of the s process is $\theta_{ss} + \Delta_s \approx 10 \cdot 10^9$ years.

6. TERMINATION OF THE s PROCESS

Nucleosynthesis of heavy stable nuclei occurring by means of the s process ends at mass numbers $A \sim 210$. Nuclei heavier than bismuth decay into isotopes of lead, which emit α particles.

The last stable nuclide in the s-process chain is ^{209}Bi . It captures a neutron, forming ^{210}Bi . The final scheme of the process, which takes place in a high-temperature neutron flux, is shown in Fig. 22 and is taken from Refs. 45 and 46. The 9^- isomeric state of ^{210}Bi at $T = 3 \times 10^8$ K lives less than a second, and thermal equilibrium of the ground and excited states of ^{210}Bi is established in about a second. Here only a few percent of ^{210}Bi nuclei remain in the 9^- state, so that to a good approximation we can consider just the two lowest states of ^{210}Bi : 1^- and 0^- . Neutron capture by ^{210}Bi in princi-

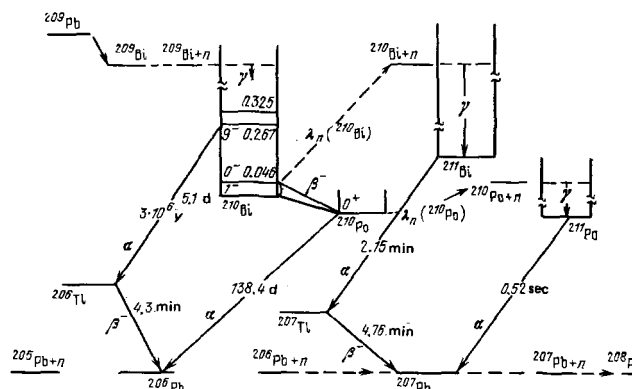


FIG. 22. Decay schemes at the end of the s-process chain.⁴⁴

ple should compete with the rate of combined β^- decay from the first two excited states of ^{210}Bi . The half-life of the ^{210}Bi ground state (5.1 days) is substantially less than the lifetime against neutron capture, and the latter can be completely neglected if we assume that ^{210}Bi decays directly to ^{210}Po . Thus, the yield of ^{210}Bi can be considered equal to zero at all times. In the nucleus ^{210}Po the excited state lies above 1 MeV and does not compete with the ground state at temperatures $\sim 10^8$ K. If the ^{210}Po lifetime against neutron capture is comparable with $T_{1/2}(^{210}\text{Po}) = 138$ days, then in the s-process chain a certain amount of ^{211}Po can be formed, which decays rapidly into ^{207}Pb ($T_{1/2} = 0.5$ sec). Consequently the system of differential equations describing the termination of the s process can be written in the form

$$\begin{cases} \frac{d(^{206}\text{Pb})}{d\tau} = -\lambda_n(^{206}\text{Pb})^{206}\text{Pb} + \lambda_\alpha(^{210}\text{Po})^{210}\text{Po} + \lambda_n(^{205}\text{Pb})^{205}\text{Pb}, \\ \frac{d(^{207}\text{Pb})}{d\tau} = \lambda_n(^{206}\text{Pb})^{206}\text{Pb} - \lambda_n(^{207}\text{Pb})^{207}\text{Pb} + \lambda_n(^{210}\text{Po})^{210}\text{Po}, \\ \frac{d(^{208}\text{Pb})}{d\tau} = \lambda_n(^{207}\text{Pb})^{207}\text{Pb} - \lambda_n(^{208}\text{Pb})^{208}\text{Pb}, \\ \frac{d(^{209}\text{Bi})}{d\tau} = \lambda_n(^{208}\text{Pb})^{208}\text{Pb} - \lambda_n(^{209}\text{Bi})^{209}\text{Bi}, \\ \frac{d(^{210}\text{Po})}{d\tau} = \lambda_n(^{209}\text{Bi})^{209}\text{Bi} - \lambda_\alpha(^{210}\text{Po})^{210}\text{Po} - \lambda_n(^{210}\text{Po})^{210}\text{Po}. \end{cases} \quad (43)$$

For convenience we shall present these differential equations in matrix form:

$$\frac{dX}{d\tau} = \Sigma X + b(\tau),$$

where

$$X = [^{206}\text{Pb}, ^{207}\text{Pb}, ^{208}\text{Pb}, ^{209}\text{Bi}, ^{210}\text{Po}], \quad (44)$$

$$b(\tau) = [\psi_{205}, 0, 0, 0, 0]$$

and the matrix Σ is given by

$$\Sigma = \begin{pmatrix} -\sigma(^{206}\text{Pb}) & 0 & 0 & 0 & \frac{\lambda_\alpha(^{210}\text{Po})}{\lambda_n(^{210}\text{Po})} \sigma(^{210}\text{Po}) \\ \sigma(^{206}\text{Pb}) & -\sigma(^{207}\text{Pb}) & 0 & 0 & \sigma(^{210}\text{Po}) \\ 0 & \sigma(^{207}\text{Pb}) & -\sigma(^{208}\text{Pb}) & 0 & 0 \\ 0 & 0 & \sigma(^{208}\text{Pb}) & -\sigma(^{209}\text{Bi}) & 0 \\ 0 & 0 & 0 & \sigma(^{209}\text{Bi}) & -\left[1 + \frac{\lambda_\alpha(^{210}\text{Po})}{\lambda_n(^{210}\text{Po})} \sigma(^{210}\text{Po})\right] \end{pmatrix}$$

The function $\psi_{205} = \sigma(^{205}\text{Pb})(^{205}\text{Pb})$ is a known function of τ which depends on the neutron-capture cross sections for all preceding nuclei in the s-process chain. It describes the yield of the initial seed nuclei ^{205}Pb in the cycle considered.

Equation (44) could be integrated easily if the matrix Σ contained constant elements. In spite of the fact that the neutron cross sections depend on the temperature and for that reason may change with time, in the first approximation they can be taken as constant. The difficulty lies in the value of the branching $\lambda_\alpha(^{210}\text{Po})/\lambda_n(^{210}\text{Po})$. This value changes with the neutron density n_n as the result of a change in $\lambda_n(^{210}\text{Po})$. The neutron density increases from zero at the beginning of the reactions which lead to liberation of neutrons, reaches some maximum at the peak of the s process, and then falls exponentially to zero with depletion of the sources of free neutrons. We can assume, however, that the neutron flux falls off with a lifetime of the same order as the time scale of the s process (the burning of helium and hydrogen). Therefore even if the neutron flux is sufficiently great that the value of $\lambda_n(^{210}\text{Po})$ could

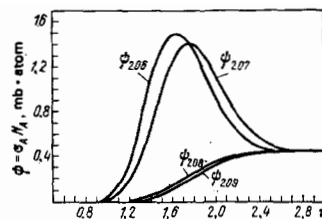


FIG. 23. Values of $\psi_A = \sigma_A N_A$ for nuclei at the end of the s-process chain.⁴⁴ The following values were used for the calculations: $\sigma_{206} = 9.6$ mb, $\sigma_{207} = 8.7$ mb, $\sigma_{208} = 0.5$ mb, $\sigma_{209} = 12.1$ mb at $kT = 30$ keV.

compete with $\lambda_\alpha(^{210}\text{Po})$, termination of the s process will occur slowly under the condition $\lambda_n \ll \lambda_\alpha$. In this case the yield of ^{211}Po can be neglected, on the assumption that the α decay of ^{210}Po into ^{206}Pb follows immediately after the neutron capture $^{209}\text{Bi} + n$.

The differential equations (44) are simplified, acquiring constant coefficients:

$$\frac{d}{d\tau} \begin{pmatrix} ^{206}\text{Pb} \\ ^{207}\text{Pb} \\ ^{208}\text{Pb} \\ ^{209}\text{Pb} \end{pmatrix} = \begin{pmatrix} -\sigma(^{206}\text{Pb}) & 0 & 0 & \sigma(^{209}\text{Bi}) \\ \sigma(^{206}\text{Pb}) & -\sigma(^{207}\text{Pb}) & 0 & 0 \\ 0 & \sigma(^{207}\text{Pb}) & -\sigma(^{208}\text{Pb}) & 0 \\ 0 & 0 & \sigma(^{208}\text{Pb}) & -\sigma(^{209}\text{Bi}) \end{pmatrix} \times \begin{pmatrix} ^{206}\text{Pb} \\ ^{207}\text{Pb} \\ ^{208}\text{Pb} \\ ^{209}\text{Pb} \end{pmatrix} + \begin{pmatrix} \psi_{205} \\ 0 \\ 0 \\ 0 \end{pmatrix}. \quad (45)$$

Clayton and Rassbach⁴⁵ obtained by numerical integration a solution of Eq. (45) which is shown in Fig. 23 in the form of the function $\psi_A(\tau)$. They showed also that the solution of the termination of the s process is not critical to the magnitude of the poorly known neutron-capture cross section of ^{208}Pb . The yields of the lead isotopes in the s process with the assumptions made earlier regarding the form of the function $\rho(\tau)$ are almost independent of σ_{208} if this quantity is small (≤ 2 mb). If $\sigma_{208} \geq 2$ mb, then the solution of the termination of the s process will depend on this quantity, but in this case it can be measured experimentally.

It is possible to show also that while small values of the exposure τ are important in calculation of the s-process yields of nuclei with $A < 200$, in the case of nuclei with $A > 200$ the principal role is played by large values of τ .⁴⁴

BRIEF CONCLUSIONS

In the initial formulation of the theory of the s process the yields of heavy nuclei ($A > 60$) along the valley of β stability were considered to be the consequence of neutron-capture chains on the assumption that the lifetimes for neutron capture were large in comparison with the lifetimes for β decay. The CFHZ theory provided a quantitative relation between the observed distribution of the yields of elements and the corresponding distribution of the neutron fluxes which bombard the iron seed nuclei, integrated over time. The correctness of this theory is confirmed by the two main features of the s process: 1) constancy of the product $\sigma_A N_A$ for small region of variation of the mass number A , and 2) the correspondence between the smooth na-

ture of the observed $\sigma_A N_A$ curve and the smooth, monotonically decreasing distribution of neutron exposures $\rho(\tau) = G \exp(-\tau/\tau_0)$.

The CFHZ solution was a mathematically correct but approximate solution of the s-process equations on the assumption of a constant neutron flux. The exact solution of these equations can be written in the form of a series expansion (the Bateman series). However, numerical summation of this series before the availability of modern computers presented great difficulties as a result of the cumbersome nature of the computations and the possible degeneracy of the neutron-cross-section values ($\sigma_m = \sigma_n$ for $n \neq m$). Recently Newman obtained an exact numerical solution of the s-process equations on the basis of the Bateman expansion which confirmed the correctness of the CFHZ approximation. At the same time this form of exact solution permitted calculation of the yields of elements to be carried out more correctly in the region of low neutron exposures.

In the comparison with experiment a difficult problem lies in the discrepancy in the experimental results on measurements of the neutron cross sections σ for various nuclides. At the same time the accuracy of the theoretical calculations of the neutron-capture cross sections turns out to be unsatisfactory in a comparison with experiment. Nevertheless at the present time it can be stated that within the experimental error of ~30% the observed yield curve of elements formed in the s process corresponds to the calculations based on the theory of the s process.

In the region of nuclei close to iron an excess of the experimental values σN_s^{exp} over the theoretical curve is observed, which can be explained by the pulsed nature of the neutron flux.

The next step in development of the theory of the s process consists of taking into account branchings due to competition of neutron capture with β decay in the s-process chain. This refinement changes (in a number of cases substantially) the track of the s process and the yields of the nuclei produced in a given branch.

In calculation of the branchings an important role is played by the temperature dependence of the lifetime of the nuclei considered for β decay. Ward, Newman, and Clayton made numerical calculations of the branchings for a number of s-process nuclei and showed that the determining parameter in such calculations is the quantity $f_- = \lambda_- / (\lambda_n + \lambda_-)$.

If we consider the various branchings as functions of the average thermodynamic conditions of the s process (the value of the neutron flux Φ , the neutron density n_n , and the temperature T), considering the cross sections, yields, and rate of β decay as known, it is possible from a fit of the observed σN ratios within each branch to calculate the average value for the s process of the temperature T , the neutron density n_n , and the neutron flux Φ . They turn out to be: $T \approx 3 \cdot 10^8$ K, $n_n \approx 1.6 \cdot 10^7$ cm⁻³, and $\Phi \approx 3.5 \cdot 10^{15}$ cm⁻² sec⁻¹.

In understanding the theory of nucleosynthesis it turns out to be important to investigate the possibility of a

pulsed neutron s process leading to formation of heavy nuclei in the interior of a star as a result of periodically repeated flares of the helium shell. In such processes the resulting neutron flux ($\Phi = 4 \cdot 10^{16}$ cm⁻² sec⁻¹, $T = 2.5 \cdot 10^8$ K) has a pulsed nature with short periods of neutron exposure (~10 years) separated by extended interpulse periods (~2500 years). R. K. Ulrich has shown that for stars of intermediate mass (~3 M_\odot) about 80 flares are required to obtain agreement with the observed abundance of the elements.

The age of nuclei formed in the s process of nucleosynthesis can be determined by means of the long-lived chronometer lutecium 176 and the nearby stable nuclides lutecium 175, hafnium 176, ytterbium 170, and tungsten 182. At the present time the data on neutron-capture cross sections in the astrophysical energy region are not sufficiently reliable. In addition the estimates of the contribution of the r process and the branching ratio of ¹⁷⁵Lu + n are not very well determined. At the same time the determination of the duration of the s process of nucleosynthesis presents significant interest from the point of view of unifying nucleosynthesis in its various manifestations. "And this is an old story but it always remains new".

In conclusion the authors express their sincere indebtedness to V. M. Chechetkin for helpful remarks.

- ¹C. Hayashi, *Prog. Theor. Phys.* **5**, 224 (1950).
- ²H. Reeves, J. Audouze, W. A. Fowler, and D. N. Schramm, *Astrophys. J.* **179**, 909 (1973).
- ³Ya. B. Zel'dovich and I. D. Novikov, *Stroenie i évolýutsiya Vselennoy* (Structure and Evolution of the Universe), Moscow, Nauka, 1975.
- ⁴S. Weinberg, *The First Three Minutes*, Plenum Press, N. Y., 1977.
- ⁵Explosive Nucleosynthesis, Ed. D. N. Schramm and W. D. Arnett, Austin and London: University of Texas Press, 1973.
- ⁶D. D. Clayton and S. E. Woosley, *Rev. Mod. Phys.* **46**, 755 (1974).
- ⁷S. W. Bruenn and A. Marroquin, *Astrophys. J.* **195**, 567 (1975).
- ⁸H. E. Suess and H. C. Urey, *Rev. Mod. Phys.* **28**, 53 (1956).
- ⁹E. M. Burbidge, G. R. Burbidge, W. A. Fowler, and F. Hoyle, *Rev. Mod. Phys.* **29**, 547 (1957).
- ¹⁰I. S. Shklovskiy, *Zvezdy: ikh rozhdenie, zhizn' i smert'* (Stars, Their Birth, Life, and Death), Nauka, Moscow, 1975.
- ¹¹W. A. Fowler, in: *Cosmology, Fusion, and Other Matters*, Ed. F. Reines, Boulder, Colorado, 1972, p. 67.
- ¹²G. S. Bisnovatyĭ-Kogan and V. M. Chechetkin, *Usp. Fiz. Nauk* **127**, 263 (1979) [*Sov. Phys. Uspekhi* **22**, 89 (1979)].
- ¹³K. Nakazawa *et al.*, *Progr. Theor. Phys.* **44**, 829 (1970).
- ¹⁴R. E. Taam and R. E. Picklum, *Astrophys. J.* **224**, No. 1, pt. 1, p. 210 (1978).
- ¹⁵V. Trimble, *Rev. Mod. Phys.* **47**, 877 (1975).
- ¹⁶B. J. Allen, J. H. Gibbons, and R. L. Macklin, *Adv. Nucl. Phys.* **4**, 205 (1971).
- ¹⁷T. G. Harrison and T. W. Edwards, *Astrophys. J.* **187**, 303 (1974).
- ¹⁸R. J. Tayler and A. S. Everest, *The Origin of the Chemical Elements*, 1975, Crane Russak. (Russ. Transl., Mir, Moscow, 1975).
- ¹⁹D. D. Clayton, W. A. Fowler, T. E. Hull, and B. A. Zimmerman, *Ann. Phys. (N.Y.)* **12**, 331 (1961).
- ²⁰H. Bateman, *Proc. Cambr. Phil. Soc.* **15**, 423 (1910).

- ²¹M. J. Newman, *Astrophys. J.* **219**, 676 (1978).
- ²²R. A. Ward and M. J. Newman, *Astrophys. J.* **219**, 195 (1978).
- ²³R. K. Ulrich, in: *Explosive Nucleosynthesis*, Ed. D. N. Schramm, and W. D. Arnett, Austin: University of Texas Press, 1973, p. 139
- ²⁴D. D. Clayton and M. J. Newman, *Astrophys. J.* **192**, 501 (1974).
- ²⁵R. L. Macklin and J. H. Gibbons, *Astrophys. J.* **149**, 577 (1967).
- ²⁶D. B. Stroud, *Astrophys. J. Lett.* **178**, L93 (1972).
- ²⁷J. A. Holmes *et al.*, *Atomic Data and Nucl. Data Tables* **18**, 305 (1976).
- ²⁸J. Conrad, Ph.D. Thesis, Heidelberg, 1976.
- ²⁹P. A. Seeger, W. A. Fowler, and D. D. Clayton, *Astrophys. J. Suppl.* **11**, 121 (1965).
- ³⁰D. D. Clayton and R. A. Ward, *Astrophys. J.* **193**, 397 (1974).
- ³¹R. L. Smith and I. J. Sackmann, Preprint, 1973.
- ³²I. Iben, Jr., *Astrophys. J.* **196**, 525 (1975).
- ³³R. A. Ward, M. J. Newman, and D. D. Clayton, *Astrophys. J. Suppl.* **31**, 33 (1976).
- ³⁴D. D. Clayton, in: *Explosive Nucleosynthesis*, Ed. W. D. Arnett, Univ. of Texas Press, 1973.
- ³⁵M. J. Newman, M. S. Thesis, Rice University, 1973.
- ³⁶A. G. W. Cameron, *Astrophys. J.* **130**, 452 (1959).
- ³⁷J. N. Bahcall, *Astrophys. J.* **139**, 318 (1964).
- ³⁸V. P. Chechev and Ya. M. Kramarovskii, *Radioaktivnost' i évolutsiya Vselennoi* (Radioactivity and Evolution of the Universe), Moscow, Nauka, 1978.
- ³⁹A. Weigert, *Z. Astrophys.* **64**, 395 (1966).
- ⁴⁰M. Schwarzschild and R. Härm, *Astrophys. J.* **150**, 961 (1967).
- ⁴¹V. L. Peterson and D. A. Tripp, *Astrophys. J.* **184**, 473 (1973).
- ⁴²J. B. Blake and D. N. Schramm, *Astrophys. J.* **197**, 615 (1975).
- ⁴³H. Reeves, *Astrophys. J.* **146**, 447 (1966).
- ⁴⁴D. D. Clayton, *Principles of Stellar Evolution and Nucleosynthesis*, N. Y., McGraw-Hill, 1968.
- ⁴⁵D. D. Clayton and M. E. Rassbach, *Astrophys. J.* **148**, 69 (1967).
- ⁴⁶M. B. Lewis, *Nucl. Data Sheets* **5**, 631 (1971).
- ⁴⁷A. G. W. Cameron, *Astrophys. J.* **65**, 485 (1960).
- ⁴⁸Yu. V. Khol'nov, V. P. Chechev, Sh. V. Kamynov, N. K. Kuz'menko, and V. G. Nedovesov, *Kharakteristiki izlucheniĭ radioaktivnykh nuklidov primenyemykh v narodnom khoz-yaystve. Otsenennye dannye. (Characteristics of Radiations of Radioactive Nuclides Used in the National Economy. Evaluated Data.)*, Atomizdat, Moscow, 1980.
- ⁴⁹J. M. Lattimer and D. M. Schramm, *Astrophys. J.* **192**, 145 (1974).
- ⁵⁰J. G. Peters, *Astrophys. J.* **154**, 225 (1968).
- ⁵¹R. G. Couch and W. D. Arnett, *Astrophys. J.* **194**, 537 (1974).
- ⁵²J. Audouze, W. A. Fowler, and D. N. Schramm, *Nature Phys. Sci.* **238**, 8 (1972).
- ⁵³E. B. Norman, *Phys. Rev. Ser. C* **21**, 1109 (1980).
- ⁵⁴V. P. Chechev and Ya. M. Kramarovskii, *Radium Institute Preprints* 107 (1979), and 129 (1980).
- ⁵⁵M. T. McCulloch, J. R. De Laeter, and K. J. R. Rosman, *Earth and Planet. Science Lett.* **28**, 308 (1976).
- ⁵⁶D. N. Schramm and G. J. Wasserburg, *Astrophys. J.* **162**, 57 (1970).

Translated by Clark S. Robinson